Technical Report
RAL-TR-97-026

Jet Shapes in Hadron Collisions: Higher Orders, Resummation and Hadronization

M H Seymour

August 1997

COUNCIL FOR THE CENTRAL LABORATORY OF THE RESEARCH COUNCILS

The Central Laboratory of the Research Councils
Library and Information Services
Rutherford Appleton Laboratory
Chilton
Didcot
Oxfordshire
OX11 0QX
Tel: 01235 445384 Fax: 01235 446403
E-mail library@rl.ac.uk

ISSN 1358-6254

RAL-97-026
hep-ph/9707338

Jet Shapes in Hadron Collisions: Higher Orders, Resummation and Hadronization

M.H. Seymour

Rutherford Appleton Laboratory, Chilton,
Didcot, Oxfordshire. OX11 0QX. U.K.

Abstract

The jet shape is a simple measure of how widely a jet's energy is spread. At present jet shape distributions have only been calculated to leading order in perturbative QCD. In this paper we consider how much these predictions should be affected by higher order perturbative corrections, by resummation of enhanced corrections to all orders, and by (power-suppressed) non-perturbative corrections. We also show that current cone-type jet definitions are not infrared safe for final states with more than three partons. Unless this situation is rectified by using improved definitions, hadron collider experiments will never be able to study the internal properties of jets with the quantitative accuracy already achieved in e^+e^- annihilation.

RAL-97-026
July 1997

1 Introduction

Hadron collisions at the Tevatron are a prolific source of high transverse momentum jets. The collider experiments, CDF and DØ, have made very high precision measurements of the inclusive jet rates[1,2], as well as the rate of n-jet events, $n \geq 2$[3,4]. At present, perturbative calculations extend to next-to-leading order (NLO) for the inclusive[5,6,7] and dijet[8,9] rates and the NLO three-jet rate is close to completion[10]. These allow quite precise studies of QCD, albeit for very inclusive quantities.

At NLO, the cross sections begin to depend on the exact definition of the jets, since the jets begin to develop internal structure. The experiments have used measures of this internal structure as a cross-check on the reliability of the calculations, as well as as a study of QCD in its own right. In fact, as we shall argue, these more exclusive event properties contain considerably more information about QCD dynamics, and make an ideal place to study QCD.

One of the most popular measures of jet structure in hadron collisions is the 'jet shape': the fraction of the jet's energy within a cone of a given size, centred on the jet direction. This has been measured by both CDF and DØ over wide ranges of phase space[11,12]. It has also been measured in photoproduction by the ZEUS collaboration[13] with essentially the same method, so in this context we can class photoproduction as a hadron collision. Making these studies in photoproduction has several advantages that offset the fact that they cannot reach as high jet E_T. The direct component of the photon means that events can be selected with very little underlying event activity. Once these are understood, one can change the kinematic cuts to bring in the resolved component and thereby study the underlying event contribution in detail. Similarly, by varying the event kinematics, one can vary the quark/gluon jet mix in a way that is under much better perturbative control than in hadron collisions.

The NLO prediction of jet rates gives a leading order (LO) prediction of the jets' internal structure[14]. Thus the calculations with which the experiments have so far compared are not expected to be terribly accurate. In this paper we discuss the extent to which this could be improved by including higher order terms in perturbation theory, by summing terms to all orders, and by including an account of hadronization. The main conclusion is that these effects together constitute a very large effect on the jet shape, and we should not be surprised if the LO calculations do not give very good fits to data.

As part of this study, we considered how reliable the jet definitions used by most experiments are for these kinds of study. The conclusion is that they are not very reliable. In order to make quantitative comparisons with theory beyond LO, this situation must be improved, either by using a cluster-type algorithm, or by a simple modification of existing cone-type algorithms. Because of this, we have not compared our results with existing experimental measurements. Our emphasis is instead on understanding what physical effects are important in determining the jet shape, how large various terms are, and how accurate a future, more complete, calculation could be.

We begin in Sect. 2 by reviewing the jet definitions in current use. In a simple approximation, we make an order by order expansion, and show that calculations for current cone-based definitions will break down at next-to-next-to-leading order (NNLO) for jet cross sections (and therefore at NLO for internal jet properties). We discuss a simple remedy, and show that this has a well-defined perturbative expansion.

Section 3 contains the real substance of the paper, in which we calculate the jet shape in several steps, with ever-increasing accuracy. We start at LO, then add higher orders in perturbation theory, followed by running coupling effects, all-orders resummation of enhanced terms and (power-suppressed) hadronization corrections.

A recent paper[15] proposed using the first moment of the jet shape as a probe of the jet shape that is less susceptible to non-perturbative corrections. In Sect. 4 we consider this in the light of our studies, and find that it is not significantly better than the full distribution.

Finally in Sect. 5 we discuss the implications of our results and the outlook for the future.

2 Jet definitions, safeness and jet cross sections

By now, collider experiments are used to comparing their data with NLO calculations. As a result, all currently-used jet definitions are infrared and collinear safe to at least NLO, i.e. when there can be up to two partons in a jet. However, this is not sufficient to guarantee a well-defined perturbative expansion, because unsafe behaviour can still arise at higher orders, i.e. when there can be many partons in a jet.

Up to now, these issues have not had to be discussed in detail. This is because the data have always been compared either with NLO calculations, or with hadron-level Monte Carlo event generators. In the former, the jet definitions are infrared and collinear safe by construction. In the latter, the typical hadronic scale ~ 1 GeV cuts off all divergent integrals, yielding finite, but fundamentally non-perturbative, cross sections.

Since in this paper we aim to calculate, at least approximately, the effect of high perturbative orders, we are forced to tackle these issues head-on. In this section, we discuss the two main jet algorithms in current use: the $k_\perp$ algorithm[16] and the iterative cone algorithm[17]. While the first is safe to all orders in perturbation theory, we shall see that the second falls into a class that we call 'almost unsafe', to be defined shortly. We show that a simple modification, proposed by Steve Ellis many years ago[18], renders it safe to all orders.

Since each experiment has defined their own slightly different version of the iterative cone algorithm, we concentrate on just one of them, the DØ algorithm[1], and only

[1]We are grateful to members of the DØ collaboration for making full details of their algorithm available to us[19].

indicate the differences with respect to other versions where relevant.

2.1 Jet definitions

All the algorithms we discuss define the momentum of a jet in terms of the momenta of its constituent particles in the same way, inspired by the Snowmass accord[20]. The transverse energy, E_T, pseudorapidity, η, and azimuth, ϕ, are given by:

$$\begin{aligned} E_{T\text{jet}} &= \sum_{i\in\text{jet}} E_{Ti}, \\ \eta_{\text{jet}} &= \sum_{i\in\text{jet}} E_{Ti}\,\eta_i / E_{T\text{jet}}, \\ \phi_{\text{jet}} &= \sum_{i\in\text{jet}} E_{Ti}\,\phi_i / E_{T\text{jet}}. \end{aligned} \tag{1}$$

We shall always use boost-invariant variables, so whenever we say 'angle', we mean the Lorentz-invariant opening angle $R_{ij} = \sqrt{(\eta_i - \eta_j)^2 + (\phi_i - \phi_j)^2}$. Also, whenever we say 'energy', we mean transverse energy, $E_T = E \sin\theta$.

2.1.1 The $k_\perp$ algorithm

We discuss the fully-inclusive $k_\perp$ algorithm including an R parameter[21]. It clusters particles (partons or calorimeter cells) according to the following iterative steps:

1. For every pair of particles, define a closeness
$$d_{ij} = \min(E_{Ti}, E_{Tj})^2 R_{ij}^2 \left(\approx \min(E_i, E_j)^2 \theta_{ij}^2 \approx k_\perp^2\right). \tag{2}$$
2. For every particle, define a closeness to the beam particles,
$$d_{ib} = E_{Ti}^2 R^2. \tag{3}$$
3. If $\min\{d_{ij}\} < \min\{d_{ib}\}$, *merge* particles i and j according to Eq. (1) (other merging schemes are also possible[16]).
4. If $\min\{d_{ib}\} < \min\{d_{ij}\}$, jet i is *complete.*

These steps are iterated until all jets are complete. In this case, all opening angles within each jet are $< R$ and all opening angles between jets are $> R$.

2.1.2 The DØ algorithm

Since this is the main algorithm we shall study, we define it in full detail. It is based on the iterative-cone concept, with cone radius R. Particles are clustered into jets according to the following steps:

1. The particles are passed through a calorimeter with cell size $\delta_0 \times \delta_0$ in $\eta \times \phi$ (in DØ, $\delta_0 = 0.1$). In the parton-level algorithm, we simulate this by clustering together all partons within an angle δ_0 of each other.

2. Every calorimeter cell (cluster) with energy above E_0, is considered as a 'seed cell' for the following step (in DØ, $E_0 = 1$ GeV).

3. A jet is defined by summing all cells within an angle R of the seed cell according to Eq. (1).

4. If the jet direction does not coincide with the seed cell, step 3 is reiterated, replacing the seed cell by the current jet direction, until a stable jet direction is achieved.

5. We now have a long list of jets, one for each seed cell. Many are duplicates: these are thrown away[2].

6. Some jets could be overlapping. Any jet that has more than 50% of its energy in common with a higher-energy jet is merged with that jet: all the cells in the lower-energy jet are considered part of the higher-energy jet, whose direction is again recalculated according to Eq. (1).

7. Any jet that has less than 50% of its energy in common with a higher-energy jet is split from that jet: each cell is considered part only of the jet to which it is nearest.

Note that despite the use of a fixed cone of radius R, jets can contain energy at angles greater than R from their direction, because of step 6. This is not a particular problem. This is essentially also the algorithm used by ZEUS (PUCELL), except that their merging/splitting threshold is 75% instead of 50%.

2.1.3 The CDF algorithm

The CDF algorithm is rather similar to DØ's, but with a different splitting procedure:

6. Any jet that has more than 75% of its energy in common with a higher-energy jet is merged with that jet: all the cells in the lower-energy jet are considered part of the higher-energy jet, whose direction is again recalculated according to Eq. (1).

7. Any jet that has less than 75% of its energy in common with a higher-energy jet is split from that jet: each cell is considered part only of the jet to which it is nearest. The directions of the two jets are then recalculated by iterating step 3.

[2]In DØ, any with energy below 8 GeV are also thrown away. For jets above 16 GeV, this makes only a small numerical difference, which is not important to our discussion, so we keep them.

2.2 Infrared and collinear safeness

The formal definition of infrared safeness is as follows:

> *An observable is infrared safe if, for* any *n-parton configuration, adding an infinitely soft parton does not affect the observable at all.* (4)

The formal definition of collinear safeness is similar:

> *An observable is collinear safe if, for* any *n-parton configuration, replacing any massless parton by an exactly collinear pair of massless partons does not affect the observable at all.* (5)

We distinguish three types of observable:

Safe: Both the above conditions are fulfilled. Cross sections are calculable order by order in perturbation theory, with hadronization effects resulting in only power-suppressed corrections.

Unsafe: One or both the conditions is violated. Cross sections are infinite in perturbation theory, signalling that they are fundamentally non-perturbative.

Almost unsafe: At first sight it appears that one or both the conditions is violated, but in fact close inspection of the algorithm shows that seemingly-minor details actually rescue its safeness. Cross sections are calculable order by order in perturbation theory, but can be rather unreliable, owing to the reliance on (typically) small parameters.

Unsafe or almost unsafe algorithms often seem perfectly safe up to a certain order in perturbation theory, after which their unsafeness reveals itself. This is the case in the iterative cone algorithm, in both its DØ and CDF variants, which are almost unsafe, despite being fully safe at NLO. As we shall shortly show, it is the fact that the particles have been passed through a calorimeter, with finite cell size and minimum energy trigger, that renders it finite. One might naively think that these minor details should make small contributions (vanishing as $E_0 \to 0$ or $\delta_0 \to 0$). However, we shall see that the energy threshold, E_0, becomes logarithmically important at NNLO, and we also argue that the cell size, δ_0, will at NNNLO. This can be dangerous for (at least) three reasons: firstly, it means that anyone making a calculation must know the very precise definitions of how the data are treated – what size and shape the calorimeter cells are, what energy they trigger at, whether they are preclustered, what preprocessing is done, etc, and must implement them in the parton-level calculation; secondly, since E_0 and δ_0 are rather small, higher-order perturbative corrections are expected to be large, as are (power-suppressed) hadronization corrections, rendering the resulting calculations unreliable; and finally in some cases, the features that render the observable finite seem so minor that they are not reported at all or considered part of the experimental set-up and 'corrected for', i.e. an almost unsafe definition is 'corrected' to an unsafe one.

This problem was first encountered by Kilgore and Giele[10]. In their calculation of three jets at NLO, they ignored details of the calorimeter, effectively setting $E_0 =$

$\delta_0 = 0$, and encountered an infrared divergence arising from the separation of three nearby partons, one of which is arbitrarily soft, into one or two jets. It turned out that in the case of the three-jet analysis they are concerned with, this situation was rendered 'almost unsafe' by an additional cut imposed by CDF – the jets should be well separated. Once this is applied, the jet cross section can be calculated order by order in perturbation theory. To our knowledge, no such cut is made in the inclusive jet cross section measurement, so unless one explicitly includes calorimeter information in the calculation it is genuinely unsafe, which would first manifest itself at NNLO.

2.3 Jet cross sections

As a concrete example of the above considerations, we calculate the inclusive jet cross section up to NNLO accuracy (up to three partons per jet). We use an extremely simple model, which is certainly too simple for quantitative predictions, but which is sufficient to illustrate the problems of infrared and collinear safeness, since it is based on the soft and collinear approximations. We consider a gluon-only world, in which the LO inclusive gluon production cross section is

$$\frac{d\sigma_0}{dp_t\, d\eta} = \frac{A^{n-3}}{p_t^n}, \tag{6}$$

where A is an arbitrary parameter with dimensions of energy, and n is of order 5 for typical p_t values of interest. We consider the double-logarithmic approximation (DLA), but with some modifications: energy-momentum is conserved at vertices according to Eq. (1); strict angular ordering is imposed. The former is two logarithms down on the DLA, while the latter is only one, but both are essential for making simple numerical treatments. In this approximation, the coupling does not run.

We also simplify the kinematics, by assuming that the $\eta \times \phi$ plane is infinite in all directions. Soft radiation is limited to a cone of size R_{max}. For concreteness, we set $R_{\mathrm{max}} = 2$, although any size considerably greater than R would give similar results.

For the sake of having a simple quantity to calculate, we consider the fully inclusive jet cross section:

$$\sigma(p_{t\mathrm{min}}) \equiv \int_{p_{t\mathrm{min}}}^{\infty} dp_t \left.\frac{d\sigma}{dp_t\, d\eta}\right|_{\eta=0}. \tag{7}$$

Clearly the LO cross section is $\sigma_0 = \frac{1}{n-1} A^{n-3}/p_{t\mathrm{min}}^{n-1}$. In all numerical results we set $p_{t\mathrm{min}} = 50$ GeV, although in this simple model, the dependence of the higher order corrections on $p_{t\mathrm{min}}$ is extremely weak.

At NLO, the DLA real contribution is:

$$d\sigma_{1R} = \sigma_0 \frac{2C_A\alpha_s}{\pi} \frac{dr}{r}\Theta(R_{\mathrm{max}} - r)\, \frac{dz}{z}\, \frac{d\varphi}{2\pi}, \tag{8}$$

and the virtual contribution is:

$$\sigma_{1V} = -\sigma_0 \frac{2C_A\alpha_s}{\pi} \left(\int_0^{R_{\mathrm{max}}} \frac{dr}{r} \int_0^1 \frac{dz}{z} - \mathcal{V} \right). \tag{9}$$

Each is separately divergent, such that the sum of the two is finite for any infrared safe jet definition. Note that we have inserted a completely arbitrary finite virtual term to emphasize the arbitrariness of the overall normalization. In the numerical plots we set $\mathcal{V} = 1$, which roughly reproduces the normalization of the full NLO calculation.

For any of the definitions above, the results are the same:

$$\sigma_1 = \frac{2C_A\alpha_s}{\pi}\int_{p_{t\min}}^{\infty} dp_{tjet}\int_0^{\infty} dp_t \frac{A^{n-3}}{p_t^n}\left(\int_R^{R_{\max}}\frac{dr}{r}\int_0^1\frac{dz}{z}\right.$$
$$\left.\Big\{\delta(p_{tjet}-zp_t)+\delta(p_{tjet}-(1-z)p_t)-\delta(p_{tjet}-p_t)\Big\}+\mathcal{V}\,\delta(p_{tjet}-p_t)\right). \quad (10)$$

The first two terms in curly brackets are contributions where the two real partons are separate jets, while the third is part of the virtual contribution – the rest has exactly cancelled the real emission contribution in which the two partons are in the same jet. Clearly the last two terms cancel as $z \to 0$, and the whole thing is finite. Integrating out p_t on the δ-functions, we obtain:

$$\sigma_1 = \frac{2C_A\alpha_s}{\pi}\int_{p_{t\min}}^{\infty} dp_{tjet}\frac{A^{n-3}}{p_{tjet}^n}\left(\int_R^{R_{\max}}\frac{dr}{r}\int_0^1\frac{dz}{z}\Big\{z^{n-1}+(1-z)^{n-1}-1\Big\}+\mathcal{V}\right) \quad (11)$$
$$= -\sigma_0\frac{2C_A\alpha_s}{\pi}\left(\log\frac{R_{\max}}{R}\Big\{\psi(n-1)+\gamma_E\Big\}-\mathcal{V}\right). \quad (12)$$

For $n = 5$, the curly bracket gives $11/6$, although of course this is nothing to do with the usual collinear $11/6$.

We can see that the DLA is not strictly a good enough approximation of this cross section, since all z values contribute equally to the final result, yielding only a single logarithm (except for large n, where $\psi(n-1) \sim \log n$). Thus we should include hard gluon corrections and gluon splitting to quark-antiquark pairs. However, it is perfectly sufficient for our illustrative purposes.

Moving to NNLO, the double-real emission cross section is given by:

$$d\sigma_{2(2)} = \sigma_0\left(\frac{2C_A\alpha_s}{\pi}\right)^2\frac{dr_1}{r_1}\Theta(R_{\max}-r_1)\frac{dz_1}{z_1}\frac{d\varphi_1}{2\pi}\frac{dr_2}{r_2}\Theta(r_1-r_2)\frac{dz_2}{z_2}\frac{d\varphi_2}{2\pi}$$
$$+\ \sigma_0\left(\frac{2C_A\alpha_s}{\pi}\right)^2\frac{dr_1}{r_1}\Theta(R_{\max}-r_1)\frac{dz_1}{z_1}\frac{d\varphi_1}{2\pi}\frac{dr_2}{r_2}\Theta(r_1-r_2)\frac{dz_2}{z_2}\frac{d\varphi_2}{2\pi}. \quad (13)$$

Although the two terms look identical, they correspond to configurations where the second gluon is emitted from the hard (first term) or soft (second term) gluon from the first splitting (i.e. they would have different colour factors if the initiating parton was a quark, C_F^2 and C_FC_A respectively). The kinematics have to be calculated accordingly.

The single-real emission cross section is given by:

$$d\sigma_{2(1)} = -\sigma_0\left(\frac{2C_A\alpha_s}{\pi}\right)^2\frac{dr_1}{r_1}\Theta(R_{\max}-r_1)\frac{dz_1}{z_1}\frac{d\varphi_1}{2\pi}\left(\int_0^{R_{\max}}\frac{dr_2}{r_2}\int_0^1\frac{dz_2}{z_2}-\mathcal{V}\right)$$
$$-\sigma_0\left(\frac{2C_A\alpha_s}{\pi}\right)^2\frac{dr_1}{r_1}\Theta(R_{\max}-r_1)\frac{dz_1}{z_1}\frac{d\varphi_1}{2\pi}\int_0^{r_1}\frac{dr_2}{r_2}\int_0^1\frac{dz_2}{z_2}, \quad (14)$$

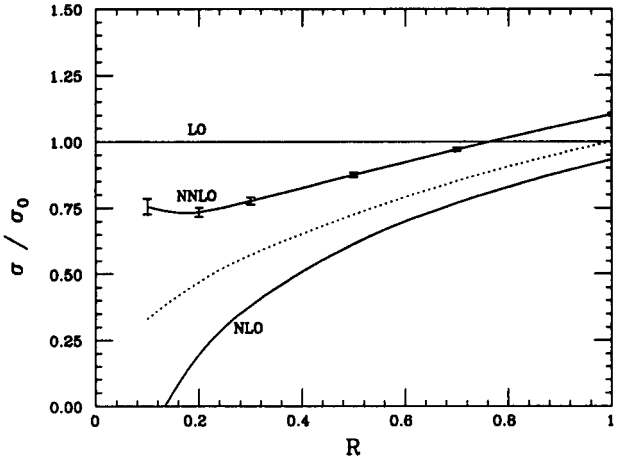

Figure 1: *The radius dependence of the inclusive jet cross section in the DØ jet algorithm with $E_0 = 1$ GeV in fixed-order (solid) and all-orders (dotted) calculations. The error bars come from Monte Carlo statistics.*

where the two terms are of the 'C_F^2' and '$C_F C_A$' type respectively. Note that we do not insert a finite virtual term in the '$C_F C_A$'-type term. Such a term could be absorbed into the running coupling, which we do not keep track of here.

Finally, the no-emission cross section is given by:

$$d\sigma_{2(0)} = \sigma_0 \left(\frac{2C_A\alpha_s}{\pi}\right)^2 \frac{1}{2} \left(\int_0^{R_{\max}} \frac{dr_1}{r_1} \int_0^1 \frac{dz_1}{z_1} - \nu\right) \left(\int_0^{R_{\max}} \frac{dr_2}{r_2} \int_0^1 \frac{dz_2}{z_2} - \nu\right), \quad (15)$$

which is of the 'C_F^2' type only.

We have implemented this as a numerical integration, and find that the cone and cluster algorithms give different results. We concentrate on the DØ algorithm, and obtain the results shown in Fig. 1. Although the absolute normalization of the corrections at each order is outside the validity of the DLA, their dependence on physical quantities, like the jet radius, should be well modelled. We see that the LO to NLO correction blows up at small R, and is not much better at NNLO (where it would diverge to positive infinity if the finite cell size, $\delta_0 = 0.1$, did not provide a cutoff). This is due to large logarithms of R, which arise at each order of perturbation theory, and would need to be summed to all orders to give accurate predictions. This is what is done in the dotted line, which is discussed in more detail in the next section.

In Fig. 2 we show the E_0 dependence of the cross section. It is clear that the dependence does not disappear as $E_0 \to 0$ at NNLO. This, then, is the proof that the DØ jet algorithm is 'almost unsafe', the safeness being rendered by the finite energy threshold of the calorimeter. Clearly in the ideal world of a perfect calorimeter, with zero threshold, we get an infinite cross section.

The strong E_0 dependence can be easily understood. It arises from configurations that have long been understood to be a problem in cone algorithms, where two partons lie somewhere between R and $2R$ apart in angle, but sufficiently balanced in energy that they are both within R of their common centre, defined by Eq. (1). This is illustrated

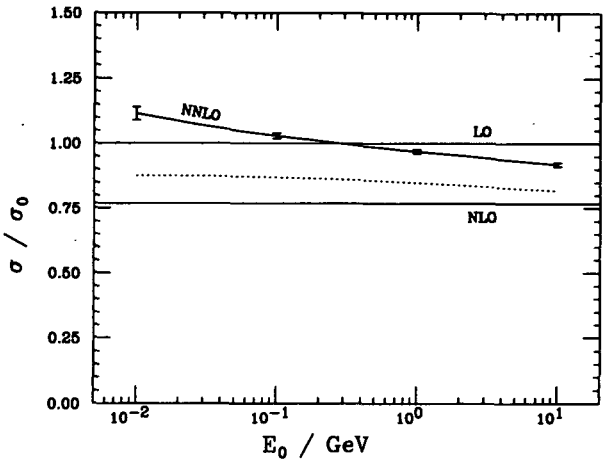

Figure 2: *The seed cell threshold dependence of the inclusive jet cross section in the DØ jet algorithm with $R = 0.7$ in fixed-order (solid) and all-orders (dotted) calculations.*

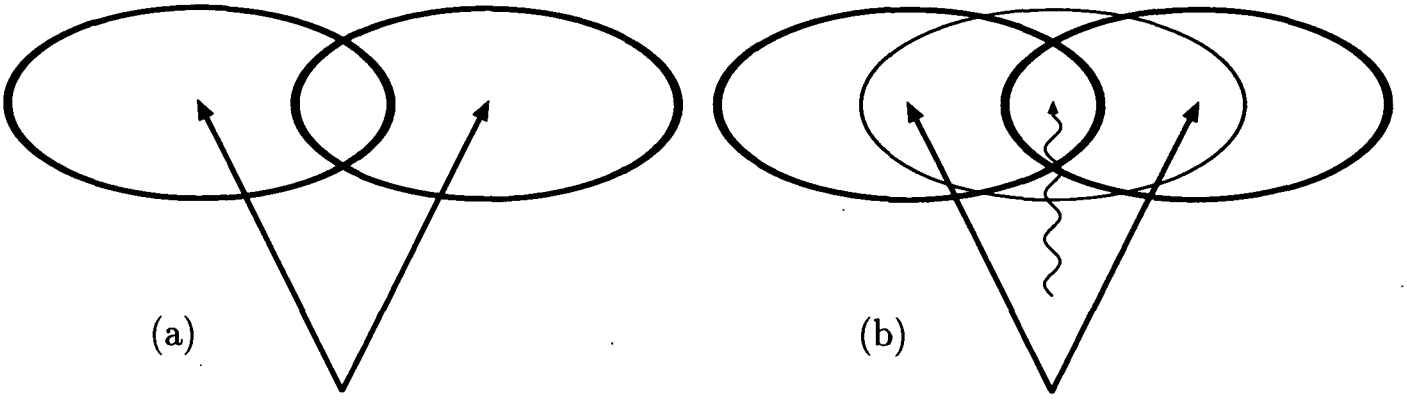

Figure 3: *Illustration of the problem region for the iterative cone algorithm. In (a), there are two hard partons, with overlapping cones. In (b) there is an additional soft parton in the overlap region.*

in Fig. 3a. According to the iterative cone algorithm, each is a separate jet, because the cone around each seed cell contains no other active cells, so is immediately stable. Although the two cones overlap, there is no energy in the overlap region, so the splitting procedure is trivial, and it is classed as a two-jet configuration.

Now consider almost the same event, but with the addition of a soft parton, close to the energy threshold E_0, illustrated in Fig. 3b. If it is marginally below threshold, the classification is as above, with the soft parton being merged with whichever hard parton it is nearest. If on the other hand it is marginally above threshold, there is an additional seed cell. The cone around this seed encloses both the hard partons and thus a third stable solution is reached. Now the merging and splitting procedure produces completely different results. In either the CDF or DØ variants the result is the same: each of the outer jets overlaps with the central one, with the overlap region containing 100% of the outer one's energy. Thus each is merged with the central one, and it is classified as a one-jet configuration.

The classification is different depending on whether or not there is a parton in the overlap region with energy above E_0. Since the probability for this to occur is $\sim \frac{2C_A}{\pi}\alpha_s \log E_T/E_0$, the inclusive jet cross section depends logarithmically on the energy threshold above which calorimeter cells are considered seed cells. Thus *the DØ jet definition is not fully infrared safe.*

In fact, having seen this problem we can see that it will become even more severe at the next higher order. Consider the probability that the soft parton splits into two fairly collinear partons. If they are greater than δ_0 apart, then they will fall into separate calorimeter cells, and neither will be above E_0, and so a one-jet configuration would be flipped back to a two-jet one. The probability for this to occur depends logarithmically on δ_0, so the inclusive jet cross section will too (at NNNLO and beyond). Thus *the DØ jet definition is not fully collinear safe.*

We should restress at this point that there is nothing special about the DØ algorithm in this regard. This is a general problem of the iterative cone type of algorithm, when used with parton directions or calorimeter cells as seed cells. We are picking on DØ simply because they were kind enough to furnish us with full details of their algorithm.

Before moving on, it is also worth recalling how the $k_\perp$ algorithm completely avoids this issue, and remains infrared safe to all orders. Merging starts with the softest (lowest relative $k_\perp$) partons. Thus in the configuration of Fig. 3b, the soft parton is first merged with whichever hard parton it is nearer. Only then is any decision made about whether to merge the two jets, based solely on their opening angle. The algorithm has completely 'forgotten about' the soft parton, and treats the configurations of Figs. 3a and 3b identically. Thus, details of the calorimeter's energy threshold become irrelevant, provided it is significantly smaller than the jet's energy.

2.4 All-orders cross section

In the previous section, we calculated the fully inclusive jet cross section in the DLA up to NNLO. In fact it is possible to sum the resulting logarithms to all orders numerically. This is done by constructing a parton shower algorithm, which iteratively applies the structure seen in the first few orders of the previous section. We have implemented such an algorithm, incorporating exactly the same conditions as in the fixed order calculations. The results were shown in Figs. 1 and 2. As anticipated, the poor behaviour in the R-dependence at small R is tamed by the resummation. Surprisingly, the same is true of the E_0-dependence, which is much milder in the all-orders result than in the NNLO result.

This can be understood as a Sudakov-type effect. Although the fraction of events with a hard emission in the problem region is small, the probability of subsequent soft emission into the overlap of the cones in those events is large, $\sim \frac{2C_A}{\pi}\alpha_s \log E_T/E_0 \sim 1$. This is precisely the logarithmic behaviour seen in the NNLO result of Fig. 2. However, when going to the all-orders result, the probability of non-emission exponentiates, and

we obtain

$$\frac{2C_A}{\pi}\alpha_s \log E_T/E_0 \longrightarrow 1 - \exp\left(-\frac{2C_A}{\pi}\alpha_s \log E_T/E_0\right) = 1 - \left(\frac{E_0}{E_T}\right)^{\frac{2C_A}{\pi}\alpha_s}, \qquad (16)$$

the much slower behaviour seen in the all-orders result of Fig. 2.

This result has a simple physical interpretation: in the 'all-orders environment', there are so many gluons around that there is almost always at least one seed cell in the overlap region and the two jets are merged to one. Recall that in our simple approximation, the coupling does not run. If we retained the running coupling, this statement would become even stronger, because the probability to emit soft gluons would be even more enhanced.

It is precisely this effect that has lead to the belief that the merging issue is a relatively unimportant numerical effect: *in the experimental environment it is.* However, expanding out the exponential of Eq. (16) as an order-by-order expansion in α_s, we obtain large coefficients at every order, and no hope of well-behaved theoretical predictions.

Thus, *if we are to study the internal properties of jets quantitatively, we must solve the overlap problem, to define jets in a perturbatively-calculable way.*

2.5 The $R_{\rm sep}$ 'solution'

It has long been realized that there is a problem with the iterative cone algorithm due to overlapping cones. A 'solution' was proposed[14] as follows: We know that in real life jets that have somewhat overlapping cones will get merged, owing to the fact that there will always be a seed cell in their overlap region. So let's *pretend* that we are using a jet definition in which they are merged even if there were no seed cells. In other words, let's modify the jet definition used in the calculation, but not in the measurement.

This modification is made by introducing an adjustable parameter, called $R_{\rm sep}$, whereby if two partons are within an angle $R_{\rm sep}R$ of each other, they are merged into one jet (provided that they are sufficiently well balanced in energy to fit into the cone of radius R around their common axis). Considerable success was claimed for this 'solution' when the same value of $R_{\rm sep}$ gave a good fit to data on both the jet cross section as a function of cone size, and the jet shape[14] (i.e. the internal structure of the jet, discussed in the next section). With the advent of more plentiful, more precise, data, it has become necessary to make $R_{\rm sep}$ a function of the event kinematics in order to fit data[22].

In our opinion, this is no solution at all. It has a multitude of problems:

- We are calculating cross sections for one observable and comparing them with measured cross sections for another. It is not clear what we learn from this. In this sense the 'NLO calculation' should be considered a model rather than a calculation of a physical cross section.

- The 'solution' does not generalize in any obvious way to higher orders. This means that we can never learn anything quantitative about the internal structure of the jets, since these are only calculable to LO. Furthermore it means that even NLO corrections to higher number of jets, such as the three-jet cross section, become uncalculable[3].

- The fact that we have 'rescued' the NLO calculation does not imply that it has any formal validity. When calculating an infrared safe quantity, non-perturbative corrections are suppressed by inverse powers of the hard scale, E_T. However, by calculating a quantity that is not infrared safe we have no way of knowing the size of non-perturbative contributions. Even in the case of almost unsafe quantities, we can only guarantee that non-perturbative corrections are suppressed by inverse powers of E_0. Since this is of order the hadronization scale, it can give rise to 100% corrections, and in any case gives corrections that do not get smaller as E_T gets bigger.

This last point means that the property of asymptotic scaling, normally expected of jet cross sections, is broken. We should not be terribly surprised if NLO calculations do not predict the energy-dependence of jet cross sections very well.

2.6 A solution

Shortly after the $R_{\rm sep}$ 'solution' was proposed, Steve Ellis proposed[18] a solution that suffers none of the problems listed above. It is a simple modification to the algorithm used in both the theoretical calculation and the experimental measurement:

> *After finding all possible jets using the seed cells, rerun the algorithm using the midpoint of all pairs of jets found in the first stage as additional seeds*[4].

This means that the results become insensitive to whether there was a seed cell in the overlap region, and hence to the energy threshold E_0. Cross sections are well-behaved and calculable order by order in perturbation theory, as shown in Fig. 4. Experimental results would be little changed by this modification (compare the all-orders results of Figs. 2 and 4), but the theoretical predictions would be enormously improved (compare the NNLO results of Figs. 2 and 4).

It should be stressed that this does not completely remove the problem of merging and splitting of overlapping cones. It merely relegates it to a procedural problem: one should state clearly the procedure one uses, and apply it equivalently to theory and experiment. Provided that that procedure uses information from all the jets in a democratic way (i.e. not keeping track of which jets came from seed cells, and which from the additional seeds), it will not spoil the improved properties of the algorithm.

[3] In this case, an additional cut on the separation of the jets renders the cross section calculable[10].

[4] To save computer time, it is sufficient to just do this for jet pairs that are between R and $2R$ apart.

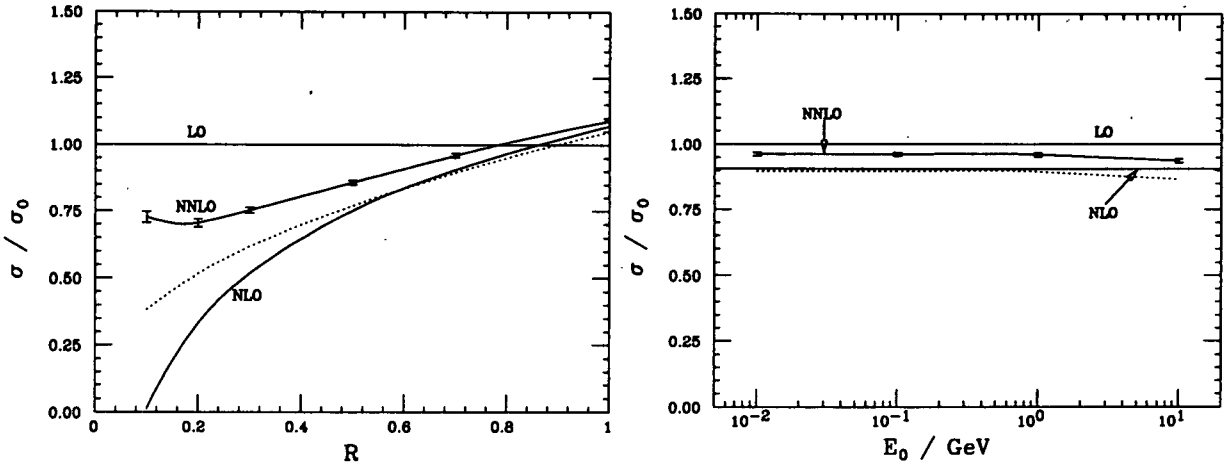

Figure 4: *The radius dependence with $E_0 = 1$ GeV (left) and seed cell threshold dependence with $R = 0.7$ (right) of the inclusive jet cross section in the improved iterative cone algorithm, in which midpoints of pairs of jets are used as additional seeds for the jet-finding, in fixed-order (solid) and all-orders (dotted) calculations.*

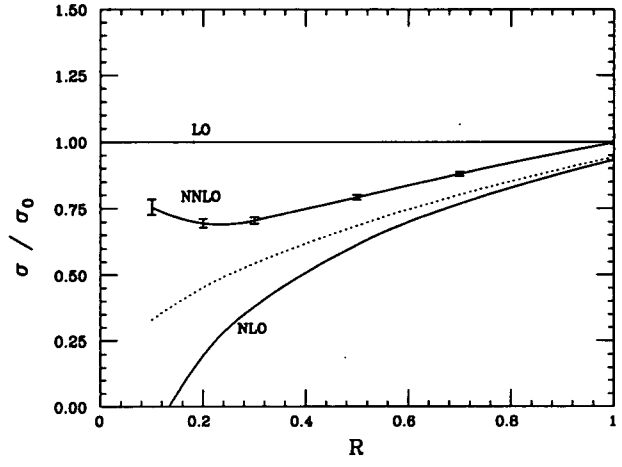

Figure 5: *The 'radius' dependence of the inclusive jet cross section in the $k_\perp$ jet algorithm in fixed-order (solid) and all-orders (dotted) calculations.*

2.7 A better solution

We finish this section by noting that using the $k_\perp$ algorithm removes these problems completely. It is fully infrared safe, and has no overlap problem, because every final-state particle is assigned unambiguously to one and only one jet. We show results in Fig. 5.

Unless there are factors of which we are unaware, abandoning the iterative cone algorithm and using the $k_\perp$ algorithm instead would be an even better solution than the previous one.

3 The jet shape

The jet shape is, at present, the most common way of resolving internal jet structure. It is inspired by the cone-type jet algorithm, but its use is not restricted to cone jets. It is defined by first running a jet algorithm to find a jet axis. The jet shape $\Psi(r;R)$ is then:

$$\Psi(r;R) = \frac{\sum_i E_{Ti}\,\Theta(r - R_{i\text{jet}})}{\sum_i E_{Ti}\,\Theta(R - R_{i\text{jet}})}, \tag{17}$$

where the sum over i can be over either all particles in the event, as used by CDF and DØ, or only those particles assigned to the jet, as used by ZEUS. We have found that using cone-type jet definitions, there is little difference between the two (less than 10% even at the jet edge). However, if the jet is defined in the $k_\perp$ algorithm, we shall see that there are strong reasons for preferring the definition in which the sum is only over those particles assigned to the jet. For now, we concentrate on the more commonly-used definition in which the sum is over all particles. Thus Ψ is the fraction of all energy within a cone of size R around the jet axis that is within a smaller cone of size r, also around the jet axis. Clearly we have $\Psi(R;R) = 1$, with $\Psi(r;R)$ rising monotonically in r.

In this paper, we prefer to work in terms of the differential jet shape:

$$\psi(r;R) = \frac{d\Psi(r;R)}{dr}. \tag{18}$$

Thus $\psi\,dr$ is the fraction of all energy within a cone of size R around the jet axis that is within an annulus of radius r and width dr, centred on the jet axis.

To define ψ in a cross sectional form, imagine defining the single-particle production cross section, differential in the particle E_T and distance from the jet axis r,

$$\frac{d\sigma}{dE_T\,dr}. \tag{19}$$

ψ is then given by:

$$\psi(r;R) = \frac{\int dE_T\; E_T \frac{d\sigma}{dE_T\,dr}}{\int_0^R dr \int dE_T\; E_T \frac{d\sigma}{dE_T\,dr}}. \tag{20}$$

3.1 Leading order calculation

As we have mentioned several times already, the NLO matrix elements for the jet cross section determine the jet shape at LO. However, it is important to note that in taking the ratio in Eq. (20), both parts should be evaluated to the same order (LO in this case). If the denominator is mistakenly evaluated to NLO, one gets artificially large renormalization scale dependence. Compare

$$\mu^2\frac{d}{d\mu^2}\,\frac{A_0\alpha_s^3(\mu)}{B_0\alpha_s^2(\mu) + B_1\alpha_s^3(\mu) + 2\beta_0 B_0\alpha_s^3(\mu)\log\mu^2/E_T^2} = -3\beta_0\frac{A_0}{B_0}\alpha_s^2(\mu) + \mathcal{O}(\alpha_s^3), \tag{21}$$

with the correct LO result,

$$\mu^2 \frac{d}{d\mu^2} \frac{A_0 \alpha_s^3(\mu)}{B_0 \alpha_s^2(\mu)} = -\beta_0 \frac{A_0}{B_0} \alpha_s^2(\mu) + \mathcal{O}(\alpha_s^3). \tag{22}$$

This mistake was made in a recent paper on jet shapes[15], which we discuss in more detail in a later section.

We can avoid having to use the virtual matrix elements at all, by noting that they only contribute to $\psi(r;R)$ at exactly $r = 0$. Thus we can calculate $\psi(r;R)$ for all $r > 0$ from the tree level matrix elements and then get the contribution at $r = 0$ from the fact that it must integrate to 1, i.e.

$$\psi(r;R) = \delta(r) + \Big(\psi_{\text{tree level}}(r;R)\Big)_+, \tag{23}$$

where $f(r;R)_+$ is a distribution defined in terms of the function $f(r;R)$ by $f(r;R)_+ = f(r;R)$ for $r > 0$ and $\int_0^R f(r;R)_+ dr = 0$. We do not therefore need a full NLO Monte Carlo program like JETRAD[7], but instead use the tree level matrix elements from NJETS[23] with our own phase space generation, adapted to be efficient for jet shapes.

It is also useful to have an analytical approximation to the matrix elements to work with. This can be done using the modified leading logarithmic approximation (MLLA), in which we have contributions from soft and/or collinear final-state emission, and soft initial-state emission.

The probability of final-state emission from a parton of type a is given by

$$dP_a = \frac{1}{2} \sum_b \frac{\alpha_s}{2\pi} \frac{d\rho^2}{\rho^2} \frac{d\varphi}{2\pi} dz\, P_{a\to bc}(z), \tag{24}$$

where φ is an azimuth around the jet axis, which we always integrate out from now on, z is the fraction of a's energy carried by b, and ρ is the opening angle between the partons. The phase space limits come from the requirements that both partons be within R of the jet axis, and the opening angle be less than $R_{\text{sep}}R$. Thus we have

$$\psi_a(r) = \sum_b \frac{\alpha_s}{2\pi} \frac{2}{r} \int_0^{1-Z} dz\, z\, P_{a\to bc}(z), \tag{25}$$

where

$$Z = \begin{cases} \frac{r}{r+R} & \text{if } r < (R_{\text{sep}} - 1)R, \\ \frac{r}{R_{\text{sep}}R} & \text{if } r > (R_{\text{sep}} - 1)R \end{cases} \tag{26}$$

Thus we obtain for a quark jet,

$$\psi_q(r) = \frac{C_F \alpha_s}{2\pi} \left[\frac{2}{r}\left(2\log\tfrac{1}{Z} - \tfrac{3}{2}(1-Z)^2\right)\right]_+, \tag{27}$$

and for a gluon jet

$$\begin{aligned} \psi_g(r) &= \frac{C_A \alpha_s}{2\pi} \left[\frac{2}{r}\left(2\log\tfrac{1}{Z} - (1-Z)^2\left(\tfrac{11}{6} - \tfrac{1}{3}Z + \tfrac{1}{2}Z^2\right)\right)\right]_+ \\ &+ \frac{T_R N_f \alpha_s}{2\pi} \left[\frac{2}{r}(1-Z)^2\left(\tfrac{2}{3} - \tfrac{2}{3}Z + Z^2\right)\right]_+, \end{aligned} \tag{28}$$

where N_f is the number of flavours.

Note that owing to the supersymmetric relations between the splitting kernels[24], for $N_f = C_A$, we have $\psi_q(r)/C_F = \psi_g(r)/C_A$. Thus even for $N_f = 5$, we expect the shape functions to be extremely similar in shape, and only differ in normalization.

There is also a contribution from initial-state radiation that happens to be inside the jet cone by chance. As shown in [25], this is essentially the same for both quark and gluon jets, and is given by a basic dipole formula (such emission can always be treated as soft), with colour factor $C \sim C_F \sim C_A/2$. We set $C = C_A/2$ for all numerical results. We have

$$dP = 4\frac{C\alpha_s}{2\pi}\, d\eta\, \frac{d\phi}{2\pi}\, \frac{d\omega}{\omega}, \tag{29}$$

where η, ϕ and ω are the pseudorapidity, azimuth around the beam direction, and energy of the gluon respectively. In terms of the jet variables, this gives

$$dP = 4\frac{C\alpha_s}{2\pi}\, \rho d\rho\, \frac{dz}{z}, \tag{30}$$

and hence

$$\psi_i(r) = \frac{C\alpha_s}{2\pi}\left[2r\left(\frac{1}{Z^2} - 1\right)\right]_+. \tag{31}$$

Note that although there is nothing special about the jet direction, as far as initial-state emission is concerned, this is singular as $r \to 0$, $r/Z^2 \to R^2/r$. This is due to the fact that soft partons anywhere in the jet will pull the jet axis away from the hard parton direction.

Since ψ_i is the same for both quark and gluon jets, it spoils the nice symmetry between quark and gluon jets, since we now have symbolically

$$\psi_q = C_F(\text{FSR}) + C(\text{ISR}), \tag{32}$$
$$\psi_g = C_A(\text{FSR}) + C(\text{ISR}). \tag{33}$$

In Fig. 6 we show the results of both the full LO matrix element integration, and our analytical approximation to it, for the $k_\perp$ algorithm ($R_{\text{sep}} = 1$). As with all the numerical results in this paper, we use the CTEQ4M parton distribution functions[26]. We see remarkably good agreement between the full result and the analytical approximation. The contribution from initial-state radiation is shown separately, and is clearly essential for this good agreement.

As R_{sep} increases, the approximation gets somewhat worse, as we see in Fig. 7, where we show results for the improved cone algorithm ($R_{\text{sep}} = 2$). This is not too surprising, as we are using the soft and collinear approximations for the kinematics, and $R_{\text{sep}} = 2$ allows hard partons to be up to almost 120° apart in azimuth. The approximation is still pretty good though (and is still very good at $R_{\text{sep}} = 1.3$ for example).

To show that the good agreement is not just fortuitous at our chosen E_T value, we also show in Fig. 8 the results at high E_T, where the quark/gluon jet mix is very different.

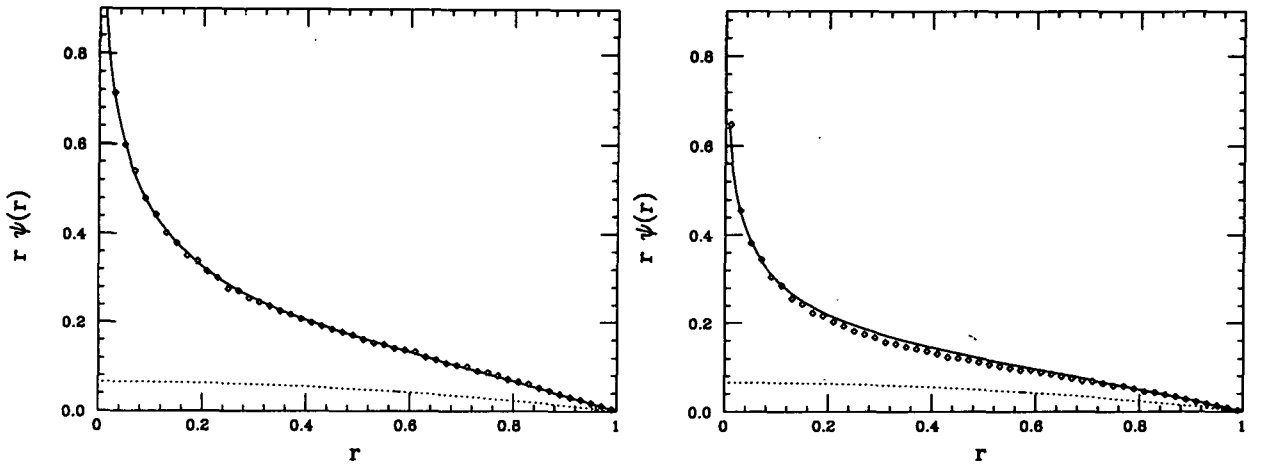

Figure 6: *The jet shape at leading order in the $k_\perp$ algorithm for a 50 GeV jet at $\eta = 0$ (left) and $\eta = 3$ (right), according to the exact tree-level matrix elements (points) and our analytical formulae (curves). The contributions of the initial-state component of the latter are shown separately as the dotted curves.*

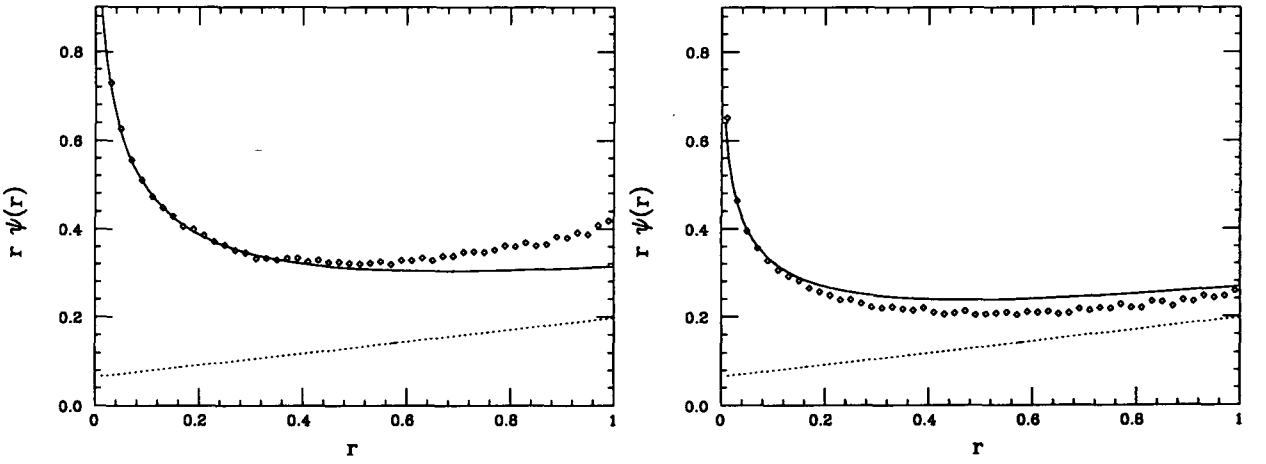

Figure 7: *As Fig. 6, but in the improved cone algorithm.*

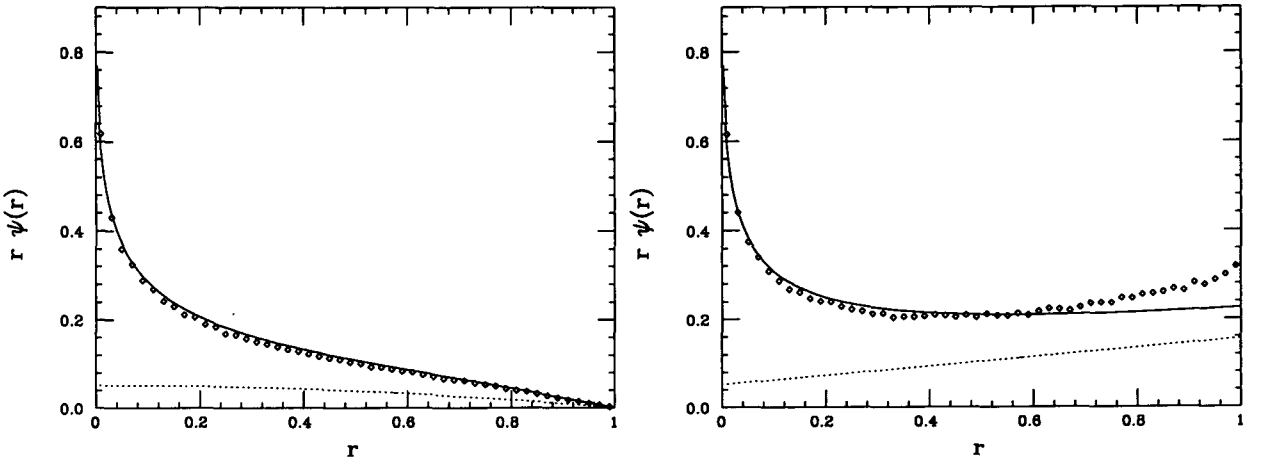

Figure 8: *The jet shape at leading order in the $k_\perp$ (left) and improved cone (right) algorithms for a 250 GeV jet at $\eta = 0$. Points and curves are as in Fig. 6.*

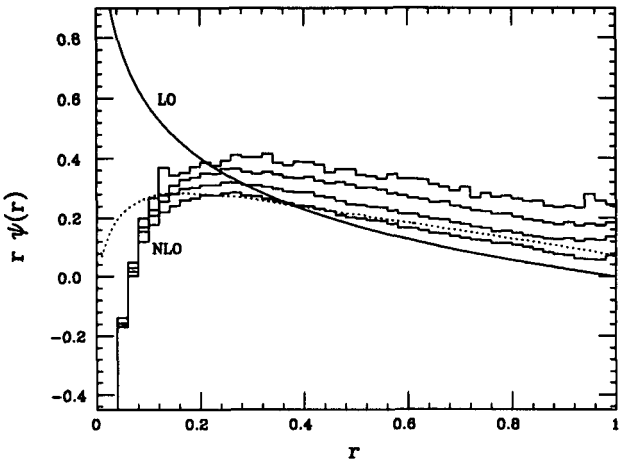

Figure 9: *The jet shape in the DØ jet algorithm in fixed-order (solid) and all-orders (dotted) calculations. In the NLO case, we use E_0 = (from top to bottom) 0.01, 0.1, 1 and 10 GeV.*

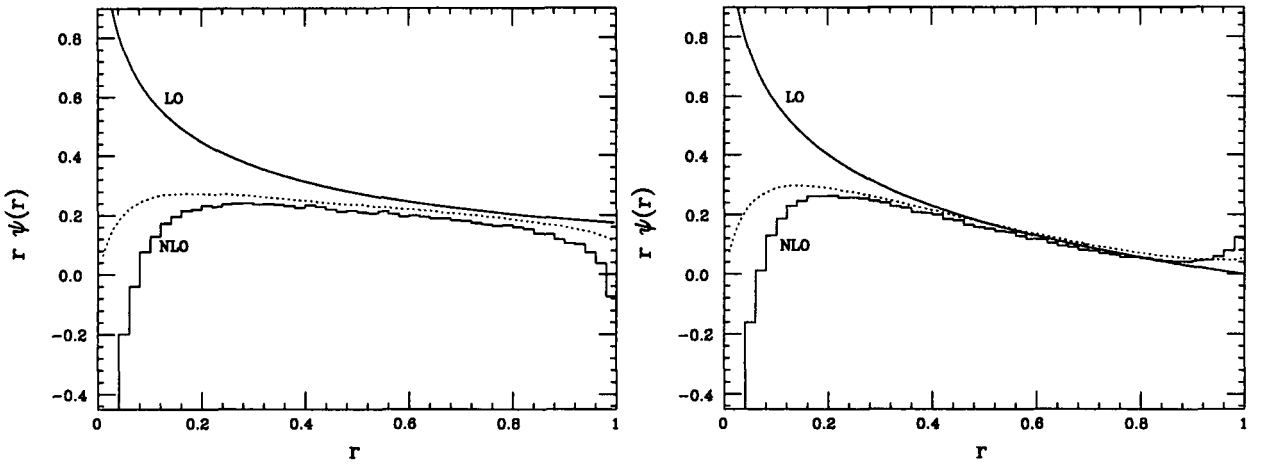

Figure 10: *The jet shape in the improved cone (left) and $k_\perp$ (right) jet algorithms in fixed-order (solid) and all-orders (dotted) calculations.*

3.2 Higher orders

Having seen that the analytical results approximate the full LO matrix element well, we move to higher orders to see how much we can improve them. We use the simple DLA of Sects. 2.3 and 2.4 to estimate the effects of higher order corrections.

In Fig. 9 we show the jet shape in the iterative cone algorithm. We see that it is strongly dependent on the seed cell threshold, as anticipated from the arguments of the previous section. We neglect it from further discussion.

In Fig. 10 we show the equivalent results in the improved cone algorithm and the $k_\perp$ algorithm. In the improved cone algorithm, the NLO corrections are rather large (recall that the normalization is outside the control of this approximation, and we should look at the shape of the corrections only). Close to the jet edge, they diverge to negative infinity,

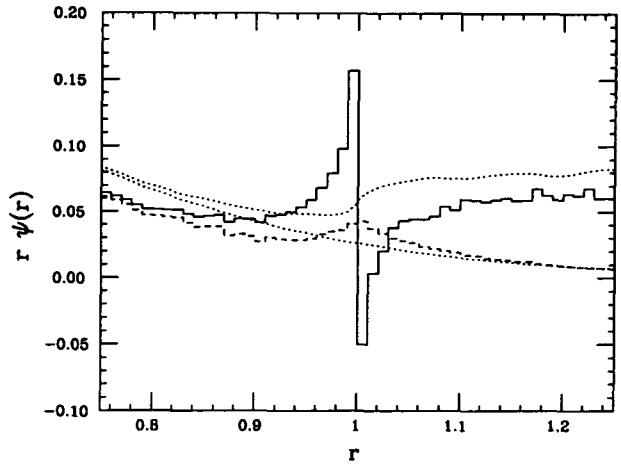

Figure 11: *The jet shape in the $k_\perp$ jet algorithm at NLO (solid and dashed) and all orders (dotted). The solid and upper dotted curve use all particles in the event, the dashed and lower dotted curve use only those particles assigned to this jet.*

a typical 'Sudakov shoulder' effect[27], analogous to the C-parameter distribution in e^+e^- annihilation for $C \sim \frac{3}{4}$. The corresponding logarithms of $(R-r)$ must be resummed to all orders for a reliable prediction. The correction in both algorithms becomes large and negative at small r, which we discuss in more detail in Sect. 3.5.

In the $k_\perp$ algorithm, the NLO corrections diverge to positive infinity near the edge of the jet. If we take a close-up view of the region $r \sim R$, as shown in Fig. 11, we see that there is a corresponding divergence to negative infinity just outside the jet edge. In the region $r \sim R$, the NLO corrections are dominated by events in which a hard gluon just outside the jet radiates a soft gluon, possibly into the jet. One can approximate this region analytically, and obtain

$$\psi(r) \sim \begin{cases} +\frac{1}{R}\log\frac{R}{R-r} & r < R \\ -\frac{1}{R}\log\frac{R}{r-R} & r > R \end{cases}, \tag{34}$$

exactly as seen in Fig. 11. Such terms would again have to be summed to all orders for a reliable prediction. We also see that even in the all-orders calculation, $\psi(r)$ changes very rapidly with r for $r \sim R$, so this region would always be difficult to model correctly.

In fact, this is an artifact of the fact that we define the jet shape using all particles in the event. If we instead use only those particles assigned to the jet, we obtain a NLO result that is continuous at $r = R$, although it still has an infinite change in slope there,

$$\psi(r) \sim \begin{cases} \frac{1}{R} - \frac{R-r}{R^2}\log\frac{R}{R-r} & r < R \\ \frac{1}{R} - \frac{r-R}{R^2}\log\frac{R}{r-R} & r > R \end{cases}, \tag{35}$$

again as seen in Fig. 11. This still indicates the formal need for a resummed calculation, but the numerical result of that resummation is a relatively minor correction, as indicated by the difference between the all orders and NLO curves. Note that the all orders calculation is smooth in this case.

To avoid these large higher order terms, we recommend that in future the jet shape be defined using *only those particles assigned to the jet by the jet algorithm.* Using this

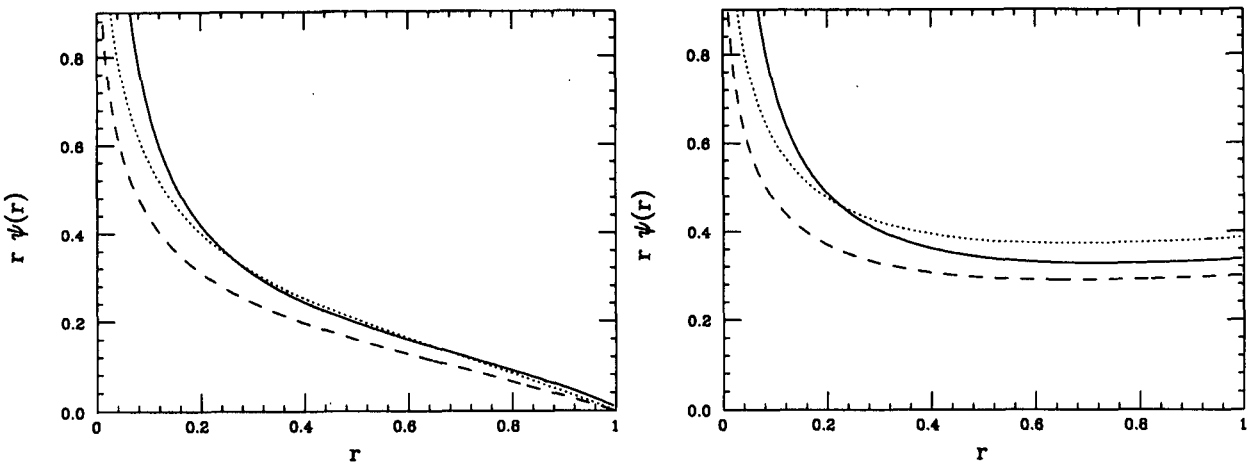

Figure 12: *Effect of running coupling on the shape of a 50 GeV jet in the $k_\perp$ (left) and improved cone (right) algorithms: $\mu = E_T$ (dashed), $\mu = E_T/4$ (dotted) and the 'best' scale defined in the text (solid).*

definition, we see that for the $k_\perp$ algorithm, the NLO curve is a good approximation to the all-orders curve for all $r \gtrsim 0.2$. For $r \lesssim 0.9$ the difference between the two definitions is small.

3.3 Scale of the running coupling

As is well known, the 'best' scale to use for the running coupling is the maximum transverse momentum of emitted gluons, relative to the axis of the emitter. For the jet shape at angle r, this is different for initial-state and final-state emission[5]. For the final-state case it is $\mu = r(1-Z)E_T$, where E_T is the transverse momentum of the jet, and for the initial-state case it is $\mu = (1-Z)E_T$.

We show the results in Fig. 12. Relative to the default scale, $\mu = E_T$, this makes a big difference, but much of that difference can be absorbed by choosing instead $\mu = E_T/4$. Then only at very small r does it become important.

3.4 Power corrections

In incorporating running coupling effects, one can go even further, by including $\alpha_s(q_t)$ inside the z integration. However, since the z integral runs from 0 to $1-Z$, this involves integrating over the Landau pole, which induces power corrections.

We basically follow the philosophy of Dokshitzer and Webber[28], and begin by

[5]This is why it is dangerous to use such schemes in exact matrix element calculations, since they do not separate emission into different components.

reviewing their method. Consider an integral

$$I_p \equiv \frac{1}{Q^{p+1}} \int_0^Q dk\, k^p\, \alpha_s(k). \tag{36}$$

Making a perturbative expansion, one obtains

$$I_{p,\mathrm{pert}} \equiv \frac{1}{p+1} \left(\alpha_s + 2\beta_0 \alpha_s^2 \left(\frac{1}{p+1} + \log \frac{\mu}{Q} \right) + \mathcal{O}(\alpha_s^3) \right), \tag{37}$$

where $\alpha_s \equiv \alpha_s(\mu)$ and $\beta_0 = (11C_A - 2N_f)/12\pi$.

If one introduces the notion of an infrared-finite coupling, then the integral

$$\bar{\alpha}_p(Q_0) \equiv \frac{p+1}{Q_0^{p+1}} \int_0^{Q_0} dk\, k^p\, \alpha_s(k), \tag{38}$$

is a well-defined, but fundamentally non-perturbative, quantity. Thus we can split the integration region of Eq. (36) in two, and obtain

$$I_p \equiv I_{p,\mathrm{pert}} + I_{p,\mathrm{pow}}, \tag{39}$$

with

$$I_{p,\mathrm{pow}} = \left(\frac{Q_0}{Q} \right)^{p+1} \frac{1}{p+1} \left(\bar{\alpha}_p(Q_0) - \alpha_s - 2\beta_0 \alpha_s^2 \left(\frac{1}{p+1} + \log \frac{\mu}{Q_0} \right) + \mathcal{O}(\alpha_s^3) \right). \tag{40}$$

Two values of $\bar{\alpha}_0(Q_0)$ were given in [28], fitted from the average value of thrust in e^+e^- annihilation:

$$\bar{\alpha}_0(2\ \mathrm{GeV}) = 0.52 \pm 0.03, \tag{41}$$

$$\bar{\alpha}_0(3\ \mathrm{GeV}) = 0.42 \pm 0.03. \tag{42}$$

These numbers actually refer to α_s defined in the physical scheme, rather than $\overline{\mathrm{MS}}$, but the difference is smaller than the errors, so we ignore it. Also, their analysis is only strictly valid when the NLO correction is included, which it is not here. Nevertheless, we use it to get a rough estimate of the importance of these corrections.

In our case, for final-state emission, we have

$$\psi(r) = \frac{1}{2\pi} \frac{2}{r} \int_0^{1-Z} dz\, z\, (P(z) + P(1-z))\, \alpha_s(zrE_T) \tag{43}$$

$$\sim \frac{2C_i}{2\pi} \frac{2}{r} \frac{1}{rE_T} \int_0^{r(1-Z)E_T} dk\, \alpha_s(k), \tag{44}$$

where $C_i = C_F$ (C_A) for a quark (gluon) jet, and the approximation corresponds to small z (i.e. small k). Thus we have

$$\psi_{\mathrm{pow}}(r) = \frac{2C_i}{2\pi} \frac{2}{r} \left(\frac{Q_0}{rE_T} \right) \left(\bar{\alpha}_0(Q_0) - \alpha_s - 2\beta_0 \alpha_s^2 \left(1 + \log \frac{\mu}{Q_0} \right) \right). \tag{45}$$

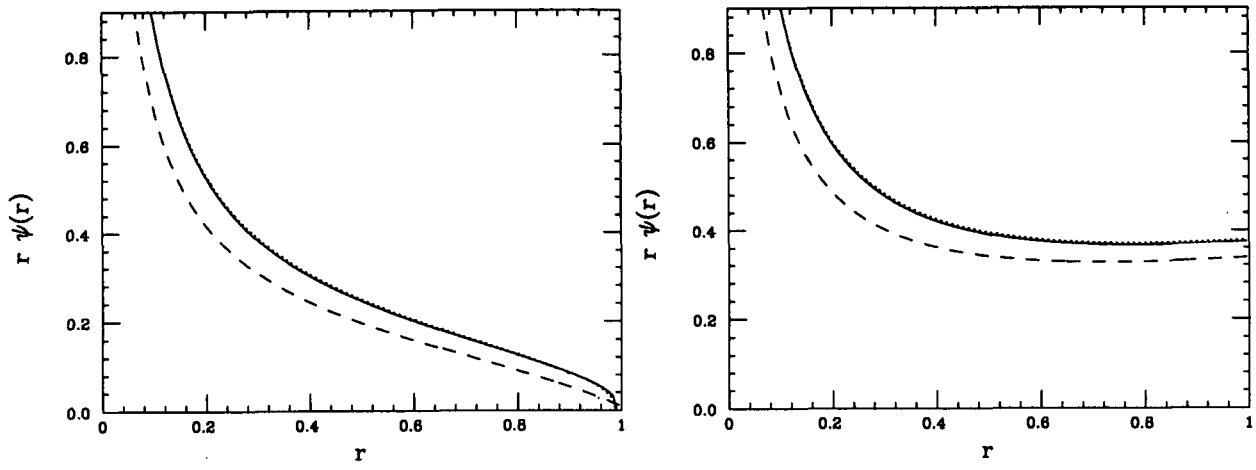

Figure 13: *Effect of power corrections on the shape of a 50 GeV jet in the $k_\perp$ (left) and improved cone (right) algorithms: no corrections (dashed), $Q_0 = 2$ GeV (solid) and $Q_0 = 3$ GeV (dotted).*

For initial-state emission, we have

$$\psi_i(r) \sim \frac{2C}{2\pi} 2r \frac{1}{E_T} \int_0^{(1-Z)E_T} dk\, \alpha_s(k), \tag{46}$$

and hence

$$\psi_{\text{ipow}}(r) = \frac{2C}{2\pi} 2r \left(\frac{Q_0}{E_T}\right) \left(\bar{\alpha}_0(Q_0) - \alpha_s - 2\beta_0 \alpha_s^2 \left(1 + \log \frac{\mu}{Q_0}\right)\right). \tag{47}$$

Note that near the core of the jet, the initial-state term is completely insignificant, while near the edge of the jet it is comparable to the final-state term.

Adding these non-perturbative corrections to our previous perturbative results, we obtain the results of Fig. 13. We see that the power corrections are sizeable, comparable to the anticipated size of NLO corrections. The curves for the two values of $\bar{\alpha}_0(Q_0)$ are completely indistinguishable – a cross-check of the consistency of the calculation.

In this context, it is relevant to question what R_{sep} really means, if anything. The value usually used, $R_{\text{sep}} = 1.3$, was obtained by fitting a LO calculation to the data, and perhaps it is double counting to continue to use this value when power corrections are included. In fact, we find that the normalization of the power-corrected LO with $R_{\text{sep}} = 1.1$ is comparable to that of LO with $R_{\text{sep}} = 1.3$.

3.5 Sudakov resummation

In the region $r \to 0$, the energy profile function develops large logarithms at all higher orders, $\sim \alpha_s^n \log^{2n-1} r$. These can be resummed to at least MLLA accuracy and, we expect, to NLLA. We work to MLLA accuracy, i.e. incorporating the $\sim \alpha_s^n \log^{2n-2} r$ terms as well, but none beyond that.

As usual in these types of calculations, it is easiest to work in terms of the total energy within r, $\Psi(r)$, rather than the energy distribution at r, $\psi(r)$, and then differentiate afterwards. Since to MLLA soft gluons do not carry away any momentum, it is straightforward to see that this is actually the same as the probability that the hard parton remains within r. To leading log accuracy, this is given by

$$P(<r) = \exp\Big(-P_1(>r)\Big), \tag{48}$$

where $P_1(>r)$ is the leading logarithm of the leading order in α_s probability that the hard parton is outside r. This is improved to MLLA accuracy simply by including the next-to-leading logarithm and running coupling in P_1, giving

$$P_{1q} = \int_{rE_T}^{RE_T} \frac{dq_t}{q_t} \frac{\alpha_s(q_t)}{\pi} \left(2\,C_F \log\frac{RE_T}{q_t} - \frac{3}{2}C_F\right), \tag{49}$$

for quark jets, and

$$P_{1g} = \int_{rE_T}^{RE_T} \frac{dq_t}{q_t} \frac{\alpha_s(q_t)}{\pi} \left(2\,C_A \log\frac{RE_T}{q_t} - \frac{1}{2}b_0\right), \tag{50}$$

for gluon jets, where $b_0 = 4\pi\beta_0 = \frac{11}{3}C_A - \frac{4}{3}T_R N_f$. Note that to this accuracy, all jet definitions are the same, and independent of $R_{\rm sep}$. This is because we can take the small r phase space limit, $Z \sim r/R$.

We obtain[6]

$$P_q(r) = \exp\left\{2C_F \log\frac{R}{r}\, f_1\left(2\alpha_s\beta_0 \log\frac{R}{r}\right) - \tfrac{3}{2}C_F\, f_2\left(2\alpha_s\beta_0 \log\frac{R}{r}\right)\right\}, \tag{51}$$

$$P_g(r) = \exp\left\{2C_A \log\frac{R}{r}\, f_1\left(2\alpha_s\beta_0 \log\frac{R}{r}\right) - \tfrac{1}{2}b_0\, f_2\left(2\alpha_s\beta_0 \log\frac{R}{r}\right)\right\}, \tag{52}$$

where $\alpha_s = \alpha_s(RE_T)$, and

$$f_1(\lambda) = \frac{1}{2\pi\beta_0\lambda}\left(\log(1-\lambda) + \lambda\right), \tag{53}$$

$$f_2(\lambda) = \frac{1}{2\pi\beta_0}\log(1-\lambda). \tag{54}$$

Differentiating with respect to r, we obtain

$$\psi_q = \frac{\alpha_s(rE_T)}{2\pi}\frac{2}{r}\left(2\,C_F \log\frac{R}{r} - \frac{3}{2}C_F\right) P_q, \tag{55}$$

$$\psi_g = \frac{\alpha_s(rE_T)}{2\pi}\frac{2}{r}\left(2\,C_A \log\frac{R}{r} - \frac{1}{2}b_0\right) P_g. \tag{56}$$

Noting that $P_q = P_g + \mathcal{O}(\alpha_s) = 1 + \mathcal{O}(\alpha_s)$, it is straightforward to see that these agree with the small-r limits of the functions derived earlier.

[6]Note that these results are identical to those of [29] for the energy-energy correlation in the back-to-back region of e^+e^- annihilation, evaluated to the same accuracy (i.e. their Eq. (10) plus the second line of Eq. (11)), except that theirs is a factor of 2 larger, because they have two jets while we have one.

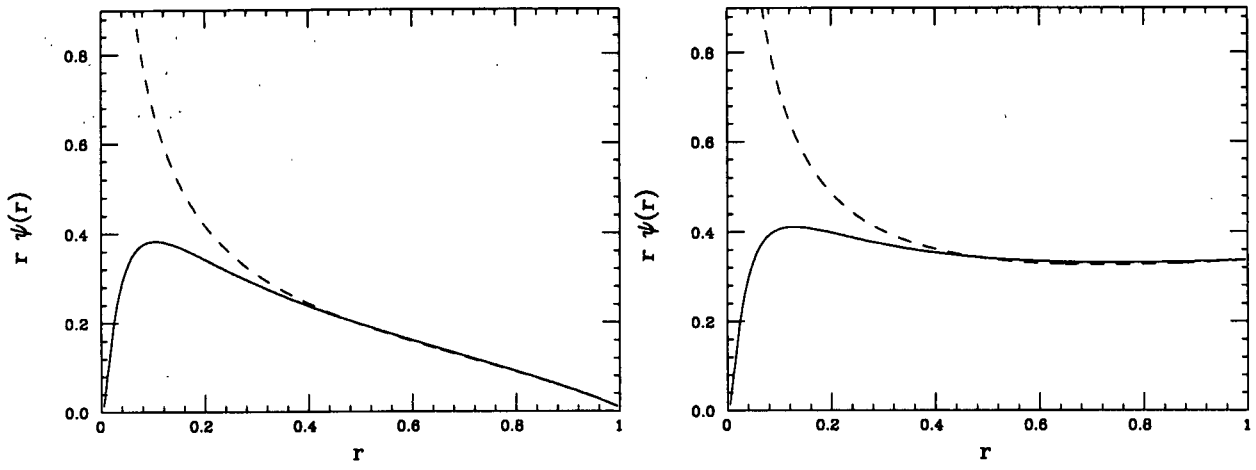

Figure 14: *Effect of resummation on the shape of a 50 GeV jet in the $k_\perp$ (left) and improved cone (right) algorithms: with (solid) and without (dashed) resummation of logarithms of R/r.*

The initial-state radiation that happens to be within the jet also contributes to MLLA accuracy, so must also be included. To fully include this to NLLA accuracy would require a more complicated analysis since, as noted earlier, the ISR and FSR contributions have different coupling effects. To MLLA however, it can be done in a straightforward way, simply by modifying $\frac{3}{2}C_F \to \frac{3}{2}C_F - C\,R^2$ and $\frac{1}{2}b_0 \to \frac{1}{2}b_0 - C\,R^2$.

We match these functions with their leading order counterparts whenever we use them (i.e. we subtract off their leading order expansions in α_s). In principle this could induce unphysical behaviour at large r, since these resummed formulae are not valid there, but in fact we find that they tend to zero like $R-r$ at $r \to R$, where the leading order result is either non-zero, for $R_{\rm sep} > 1$, or has the same behaviour, for $R_{\rm sep} = 1$. Thus we do not have to take any special precautions at the edge of phase space.

We show the results in Fig. 14, where the resummation is seen to be crucial at small r, taming the unphysical rise in ψ, but it does not make a great deal of difference for $r > 0.2$, where most of the data are. Note that our result should not be trusted for very small r, i.e. for $\lambda \sim 1$, since higher order effects such as the emission of a pair of gluons with balancing transverse momentum must then become important[30]. This is signalled by the divergence of f_1 and f_2 at $\lambda = 1$.

One might expect that the integral inside the form factor receives power corrections, as has been observed for some event shapes in e^+e^- annihilation[31]. However, following the method of [31], one finds only sources of $1/E_T^2$ corrections in our case, which are insignificant relative to the $1/E_T$ terms already discussed. Thus we do not bother including them. We do however assume that the leading $1/E_T$ corrections from final-state radiation are suppressed by the perturbative form factor, since soft gluon emission should only be enhanced at small angles in events in which the jet initiator has remained at a small angle itself.

Combining the power corrections with the all-orders resummation we obtain our

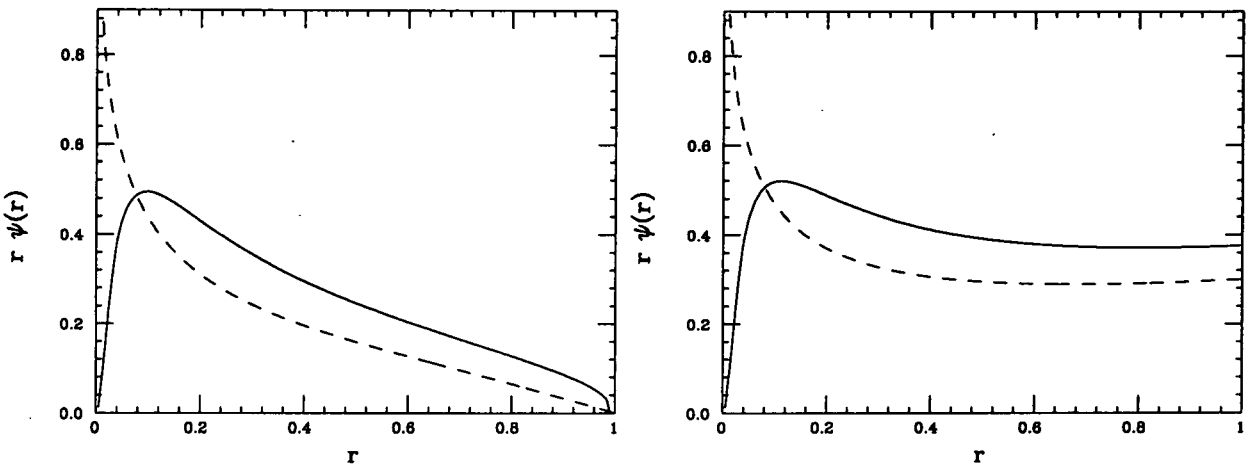

Figure 15: *Total effect of running coupling, power corrections and resummation on the shape of a 50 GeV jet in the $k_\perp$ (left) and improved cone (right) algorithms: LO (dashed) and with everything (solid).*

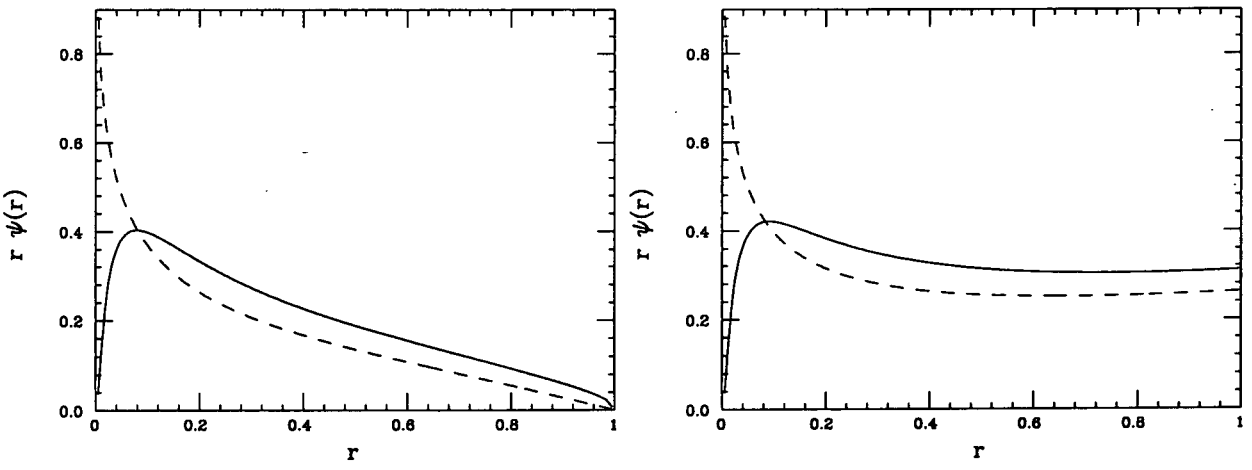

Figure 16: *As Fig. 15 but for a 100 GeV jet.*

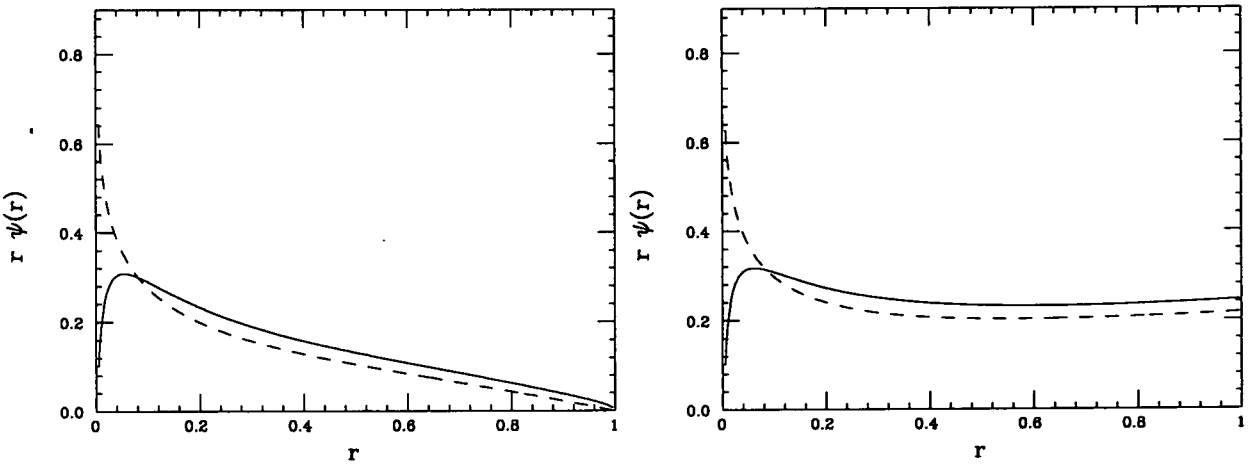

Figure 17: *As Fig. 15 but for a 250 GeV jet.*

final results for the jet shape at the Tevatron, shown in Figs. 15–17. Also shown for comparison are the original leading order results. At $E_T = 50$ GeV, the combined effect of all the corrections we have considered roughly doubles the amount of energy near the edge of the jet. Even at high transverse energy, $E_T = 250$ GeV, it is increased by about 50%, although most of this is accounted for by running coupling effects.

4 The radial moment

It was recently proposed that the first moment of the jet shape, $\langle r \rangle$, is a good measure of perturbative QCD. Since this is simply the area under the curves of the previous section, we are in a good position to calculate $\langle r \rangle$ and compare our results with those of [15].

We can again make the simple analytical approximation of the previous section, and obtain

$$\langle r \rangle_q = \frac{C_F \alpha_s}{2\pi} R \left[8 \log R_{\rm sep} + 2 + 6/R_{\rm sep} - 3R_{\rm sep} - 2/R_{\rm sep}^2 \right] + \langle r \rangle_{ISR}, \tag{57}$$

$$\langle r \rangle_g = \frac{C_A \alpha_s}{2\pi} R \left[8 \log R_{\rm sep} + \tfrac{2}{3} + 8/R_{\rm sep} + \tfrac{4}{3}/R_{\rm sep}^3 - \tfrac{2}{5}/R_{\rm sep}^4 - 4/R_{\rm sep}^2 - \tfrac{14}{5} R_{\rm sep} \right]$$
$$+ \frac{T_R N_f \alpha_s}{2\pi} R \left[\tfrac{8}{3} - 4/R_{\rm sep} + 4/R_{\rm sep}^2 - \tfrac{8}{3}/R_{\rm sep}^3 + \tfrac{4}{5}/R_{\rm sep}^4 - \tfrac{2}{5} R_{\rm sep} \right] + \langle r \rangle_{ISR}, \tag{58}$$

$$\langle r \rangle_{ISR} = \frac{C \alpha_s}{2\pi} R^3 \left[4R_{\rm sep}^2 - \tfrac{4}{3} R_{\rm sep}^3 - \tfrac{4}{3} \right]. \tag{59}$$

Note that these are the same as in [15], except that they neglected the initial-state contribution[7]. For $R = 1$, $R_{\rm sep} = 1.3$, this gives a contribution of 25% to gluon jets and 45% to quark jets, so is clearly important in determining the E_T-dependence of the jet shape.

In Fig. 18 we show the dependence of our results on the renormalization and factorization scales. We see that again the analytical approximation works very well, agreeing with the exact matrix element calculation to within 5% everywhere, and considerably better at low E_T where the data lie at present, so we use it for the remainder of this section. In this approximation, the only dependence on the factorization scale is the changing mix of quark and gluon jets. Note that our scale-dependence is overall much smaller than that of [15], owing to the fact that we consistently truncate at LO, whereas they include a partial set of NLO terms, as illustrated in Eqs. (21) and (22).

Turning to the improvements we made for the jet shape distribution in the previous section, we find that in the radial moment there are no large logarithms to resum, so neither the running coupling nor the Sudakov resummation make any formal difference to the results (although it can be seen from Figs. 12 and 14 that they do make considerable numerical difference). However, power corrections are extremely important, as discussed

[7]This comment applies to the analytical results with which they illustrate their argument. All their numerical results use the exact matrix elements so do correctly include this contribution.

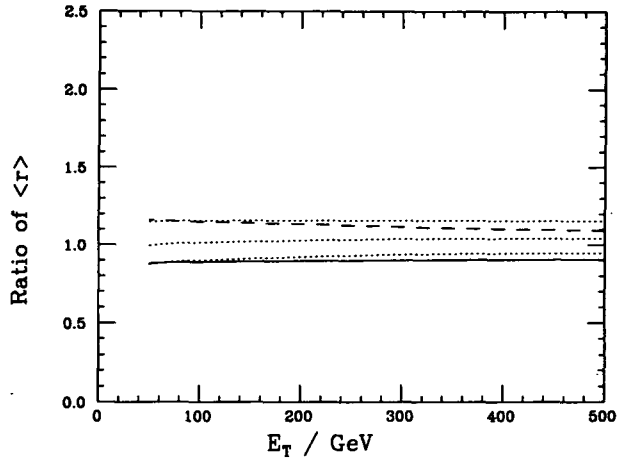

Figure 18: *Dependence of the radial moment on the factorization and renormalization scales, μ. Solid = ratio of $\mu = E_T$ to $\mu = E_T/2$, dashed = $\mu = E_T/4$ to $\mu = E_T/2$, with $R = 0.7$, $R_{\rm sep} = 2$, and CTEQ4M pdfs with $\alpha_s(M_Z) = 0.116$. The dotted curves are the same but with the numerator evaluated using our analytical approximation.*

in [15]. Using our approach, we can estimate the power corrections as

$$\langle r \rangle \sim \frac{4C_i}{2\pi} \int_0^R dr \int_0^1 dz\, \alpha_s(zrE_T) \tag{60}$$

$$= \frac{4C_i}{2\pi} \int_0^{RE_T} \frac{dk}{E_T} \alpha_s(k) \log \frac{RE_T}{k}, \tag{61}$$

and hence

$$\langle r \rangle_{\rm pow} = \frac{4C_i}{2\pi} \frac{1}{2\beta_0 \alpha_s(RE_T)} \left(\frac{Q_0}{E_T}\right) \left(\bar{\alpha}_0(Q_0) - \alpha_s - 2\beta_0 \alpha_s^2 \left(1 + \log \frac{\mu}{Q_0}\right)\right). \tag{62}$$

From the initial-state contribution, we only find $1/E_T$ corrections that are not enhanced by the extra logarithm, so we can neglect them. Comparing our result with [15], we find a big difference. Their power correction is $\sim 1/\langle r \rangle_{LO} \sim 1/C_i \alpha_s(E_T)$ while ours is $\sim C_i/\alpha_s(E_T)$. Therefore their hadronization corrections are smaller for gluon jets than quark jets, in contrast with what one would expect from a simple colour tube model[32], in which a gluon jet is attached to two colour tubes and a quark jet is attached to one. Thus one would naïvely expect twice the correction for a gluon jet than for a quark jet. This is in agreement with what we find, $\langle r \rangle_{g\rm pow}/\langle r \rangle_{q\rm pow} = C_A/C_F = 9/4$. This can be expected to affect the E_T dependence, since the flavour mix changes considerably with E_T.

We have repeated the fit to the data collated in [15] using our results. Following their approach, we multiply the LO prediction by a K factor that is allowed to vary in the fit. Fixing $R_{\rm sep} = 1.3$ and $\mu = E_T/2$, we obtain a good fit to the data, as shown in Fig. 19. Setting $Q_0 = 2$ GeV, we obtain $K = 0.54 \pm 0.06$ and $\bar{\alpha}_0(2\text{ GeV}) = 0.55 \pm 0.06$. This is in very good agreement with the results of [28], particularly bearing in mind that our perturbative results are only LO while theirs were NLO. We also get good agreement for $Q_0 = 3$ GeV, with $K = 0.52 \pm 0.06$ and $\bar{\alpha}_0(3\text{ GeV}) = 0.44 \pm 0.04$. In both cases the values of K and $\bar{\alpha}_0$ are strongly anticorrelated.

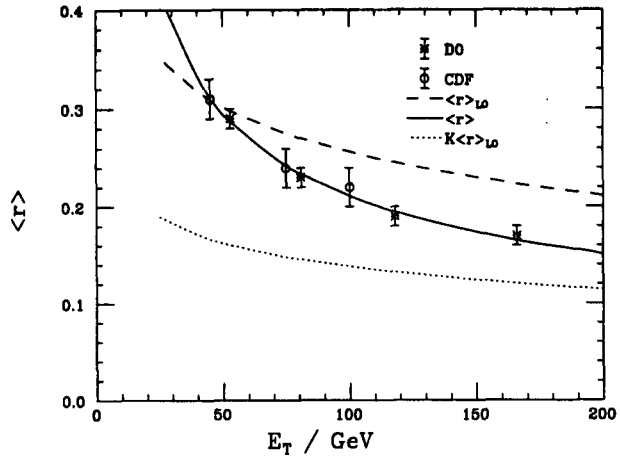

Figure 19: *The radial moment at the Tevatron. Data are from [11,12,15]. The dashed curve is the leading order perturbative result, with* $R = 1$, $R_{\rm sep} = 1.3$ *and CTEQ4M pdfs with* $\alpha_s(M_Z) = 0.116$. *The solid curve is our fit to the data. The dotted curve is the perturbative component of the fit.*

It is interesting to note that although our LO results are considerably larger than those in [15], presumably because of the partial set of NLO terms they include, our K factor comes out almost identical to theirs. This is presumably a reflection of the fact that the E_T dependencies of the power-suppressed terms are considerably different owing to the different flavour dependencies. If our perturbative contribution is forced to be as small as theirs, the resulting $\bar{\alpha}_0$ does not agree with [28].

One might worry about how far from unity the fitted value of K is. However, we have already argued in the previous section that with current jet definitions one expects large uncertainties and large higher order corrections, so we are not unduly worried. In fact in this context it is worth pointing out that we can get an equally good quality of fit, with comparable $\bar{\alpha}_0$ values, for any $R_{\rm sep}$ between 1 and 2. Any change in $R_{\rm sep}$ is compensated by a change in K in the fit. It is hard to draw any quantitative conclusions without improved jet definitions and a full NLO calculation.

5 Summary and discussion

In this paper we have tried to examine all the important effects associated with predicting the jet shape distribution in hadron collisions. In doing so, we are examining the details of how a hard parton turns into a jet of hadrons. We have estimated that large corrections arise from high orders in perturbation theory and from non-perturbative effects. Traditionally, this has been regarded as a reason to shy away from looking inside jets, but we would like to advocate exactly the opposite view: the parton→hadrons transition is one of the most interesting outstanding questions in QCD, and it is precisely because these effects are large that we should look inside jets to study them. Hadron collisions make a perfect place to make such studies, because they are a source of high rates of jets over a very wide range of jet scales in the same experiment.

However, we have also emphasized the importance of infrared safe jet definitions. These are essential, because in order to study the onset of non-perturbative effects, we must have a perturbative 'background' that is well understood and under control. If we use an infrared unsafe jet definition, then the whole process is non-perturbative, and we have no 'solid ground' to start from. Furthermore, if one wants to use the jets for perturbative jet physics, for example to measure the inclusive jet cross section, it is important that the definition be safe to all orders, not just the order to which the theoretical calculations are carried out. With an infrared safe jet definition, non-perturbative corrections are guaranteed to be suppressed by (at least) one power of '1 GeV'$/E_T$, while if unsafe behaviour arises at any higher order there are no such guarantees. In particular, in an unsafe (or 'almost unsafe') algorithm, there is no reason to expect the cross section to show the same scaling with energy as the perturbative calculation.

We have critically examined the current norm in hadron collider jet definitions: the iterative cone algorithm. We have shown that it becomes unsafe at next-to-next-to-leading order for jet cross sections, which means next-to-leading order for internal jet properties. Since next-to-leading order is the minimum required for quantitative analysis, this means that using current jet definitions one can never probe the internal structure of a jet in a quantitative way. We therefore recommend that:

- Experiments should abandon cone-based algorithms, and use the version of the $k_\perp$ algorithm adapted to hadron collisions[16,21].
- If for some reason this is not possible, they should improve the cone-based algorithms as discussed in Sect. 2.6. It would help ensure that the same definition is used in theory and experiment if the experiments made their jet algorithms publicly available.

We also discussed a 'solution' that purported to cure these problems: the introduction of an $R_{\rm sep}$ parameter. In our view, this has obscured the whole subject for several years, by giving the impression that leading order perturbative QCD gave a good description of data on the internal structure of jets, when we have absolutely no right to expect it to. We have shown that higher order corrections and non-perturbative corrections can each be expected to be as large as 50% in some phase space regions, so it would be a miracle if the leading order predictions gave a good fit to data. At any given phase space point, we can mask all our ignorance simply by adjusting $R_{\rm sep}$, and only when we study the dependence on the jet kinematics do we get found out. This is illustrated in Fig. 19 for example, where it is clear that any one of the points could be fit by varying $R_{\rm sep}$ (i.e. by shifting the dashed curve up or down by an arbitrary amount) but the only ways to simultaneously fit all of them are either to abandon all pretence that $R_{\rm sep}$ is related to the jet definition, and just treat it as a fit parameter that is allowed to vary as an arbitrary function of the jet kinematics, or to realize that there is more to the internal structure of jets than leading order perturbative QCD. It is precisely what this 'more' is, that we have tried to explore in this paper.

In addition to the jet definition, we also discussed an ambiguity in the jet shape

definition. In some experiments it is defined using all particles (that are close enough to the jet axis) in the event, while in others it is defined using only those particles that are assigned to the jet by the jet definition. For cone-type jet definitions there is little to choose between them, but in the $k_\perp$ algorithm the next-to-leading order corrections are much better behaved in the latter case than the former (see Sect. 3.2). We therefore recommend that:

- Experiments define the jet shape distribution using only those particles assigned to the jet, and no other particles that happen to be nearby.

It is hoped that full next-to-leading order calculations will soon be available for the jet shape, enabling quantitative analyses to be made for the first time. Next-to-leading order has the advantage of modelling effects that happen near edge of the jet – merging and splitting issues in cone algorithms and the raising of the 'kinematic zero' at $r = R$ in the $k_\perp$ algorithm. It also has a much better defined normalization, so the difference between the data and the predictions will provide a strong constraint on non-perturbative corrections.

We have made an approximate calculation of the next-to-leading order corrections. Although it is too crude to predict the expected normalization, it should provide a good model of the kinematic effects. We therefore predict that when the full calculation is made, the following features will be found:

- The corrections in the iterative cone algorithm will be infrared unsafe (in the method of [10] this will manifest itself as an s_{min} dependence analogous to our E_0 dependence in Fig. 9).
- In the improved cone algorithm, the corrections will be large and negative, diverging to negative infinity at both small and large r.
- In the $k_\perp$ algorithm, the corrections will also diverge to negative infinity at small r. At large r the results will depend critically on whether all particles are used (in which case they will diverge to positive infinity), or only those particles in the jet (in which case they will have a small cusp at $r = R$).

Once the next-to-leading order calculation is available, by far the largest missing effects will be (at small r) higher order terms enhanced by logarithms of r and (at medium to large r) non-perturbative power-suppressed corrections. In this paper we have shown how to resum the large logarithms to modified leading logarithmic accuracy (i.e. summing terms like $\alpha_s^n \log^{2n-1} r$ and $\alpha_s^n \log^{2n-2} r$ to all orders in α_s), and we expect that this can be extended to a full next-to-leading logarithmic resummation. We have also calculated in the Dokshitzer-Webber approach the effect of power-suppressed terms on the jet shape distribution. Although these depend on fundamentally non-perturbative parameters, in their approach these parameters are postulated to be universal, and have already been measured in e^+e^- annihilation.

It is important to note that both of these effects are independent of the precise details of the jet definition (in the $R_{\rm sep}$ language, they are completely $R_{\rm sep}$-independent). Therefore it would be straightforward to combine them with the next-to-leading order calculation, when available.

One source of power-suppressed terms that we have not discussed is the 'underlying event', the soft hadrons that are sprayed around the event by secondary interactions between the hadron remnants. As estimated in [15,33], this is less important than the hadronization corrections that we have considered in this paper. Nevertheless, since it has the same energy-dependence as the hadronization corrections, it cannot easily be separated out, and at some level it must be understood before fine details of the hadronization can be extracted. Jet shape analyses in photoproduction could prove crucial from this point of view since one can 'tune' the underlying event in or out by selecting different dijet kinematics. Unfortunately however, it seems that next-to-leading order calculations for photoproduction are more distant than for hadron collisions.

In Ref. [15], the first moment of the jet shape distribution was proposed as a good measure of jet shape. From the perturbative point of view, it has the disadvantage that power corrections are larger in the radial moment ($\sim 1/\alpha_s E_T$) than in the full distribution ($\sim 1/rE_T$). One advantage of the radial moment is that it is a single quantity that can be plotted as a function of the jet kinematics, rather than a whole distribution. It is also free from large logarithmic corrections. However, both these statements can be equally applied to some measure such as the integral of $r\psi(r)$ from 0.25 to 0.75, which has power corrections that are smaller by a factor α_s. In our opinion, either approach throws away important dynamic information that is contained in the shape of the distribution, and one would be much better off simply measuring $\psi(r)$ over as wide a range of r and event kinematics as possible, and then possibly neglecting the extreme regions of small and large r in the comparison with theory, exactly as e^+e^- annihilation experiments do with event shapes.

Despite our misgivings about the quality of the jet definition, and the use of only a leading order calculation, we made a fit to the experimental data on the radial moment. It is encouraging that the resulting non-perturbative parameter is in agreement with that extracted from e^+e^- annihilation data. If confirmed with a full next-to-leading order perturbative calculation, this would be a highly non-trivial test of the universality implicit in the Dokshitzer-Webber approach. In particular, these coefficients have never been measured in gluon-induced jets.

There has been a rapidly-increasing interest in the internal structure of jets in recent years, which is now being spurred on by the promise that the next-to-leading order corrections are imminent. We believe that jet studies in hadron colliders are at a similar point to e^+e^- annihilation before the Z factories, and that we are about to enter a new era of high precision predictions and measurements of a wide range of jet properties. To realize this potential we need close collaboration between theorists and experimenters to define observables that are sensitive to the interesting physics and feasible to calculate, and measure, accurately. The jet shape distribution considered in this paper is only scratching the surface.

References

1. F. Abe *et al.*, CDF Collaboration, Phys. Rev. Lett. 77 (1996) 438.

2. G.C. Blazey, for the DØ Collaboration, in Proceedings of the 31st Rencontres de Moriond: QCD and High-energy Hadronic Interactions, Les Arcs, France, 1996, p. 155.

3. F. Abe *et al.*, CDF Collaboration, Phys. Rev. Lett. 77 (1996) 5336, erratum *ibid.* 78 (1997) 4307; Phys. Rev. D54 (1996) 4221.

4. S. Abachi *et al.*, DØ Collaboration, Phys. Rev. D53 (1996) 6000.

5. F. Aversa, P. Chiappetta, M. Greco and J.P. Guillet, Phys. Rev. Lett. 65 (1990) 401; Z. Phys. C46 (1990) 253;
   F. Aversa, P. Chiappetta, L. Gonzales, M. Greco and J.P. Guillet, Z. Phys. C49 (1991) 459.

6. S.D. Ellis, Z. Kunszt and D.E. Soper, Phys. Rev. Lett. 62 (1989) 726; Phys. Rev. D40 (1989) 2188; Phys. Rev. Lett. 64 (1990) 2121.

7. W.T. Giele, E.W.N. Glover and D.A. Kosower, Nucl. Phys. B403 (1993) 633; Phys. Rev. Lett. 73 (1994) 2019.

8. S.D. Ellis, Z. Kunszt and D.E. Soper, Phys. Rev. Lett. 69 (1992) 1496;
   S.D. Ellis and D.E. Soper, Phys. Rev. Lett. 74 (1995) 5182.

9. W.T. Giele, E.W.N. Glover and D.A. Kosower, Phys. Rev. D52 (1995) 1486.

10. W.T. Giele and W.B. Kilgore, Phys. Rev. D55 (1997) 7183;
    W.B. Kilgore, 'Next-to-leading Order Three Jet Production At Hadron Colliders', hep-ph/9705384.

11. F. Abe *et al.*, CDF Collaboration, Phys. Rev. Lett. 70 (1993) 713.

12. S. Abachi *et al.*, DØ Collaboration, Phys. Lett. B357 (1995) 500.

13. M. Derrick *et al.*, ZEUS Collaboration, contribution to the XXVIII ICHEP, Warsaw, 1996, pa 02-043; DESY preprint in preparation.

14. S.D. Ellis, Z. Kunszt and D.E. Soper, Phys. Rev. Lett. 69 (1992) 3615.

15. W.T. Giele, E.W.N. Glover and D.A. Kosower, 'Jet Investigations Using The Radial Moment', hep-ph/9706210.

16. S. Catani, Yu.L. Dokshitzer, M.H. Seymour, B.R. Webber, Nucl. Phys. B406 (1993) 187.

17. F. Abe *et al.*, CDF Collaboration, Phys. Rev. D45 (1992) 1448.

18. S.D. Ellis, private communication to the OPAL Collaboration;
D.E. Soper and H.-C. Yang, private communication to the OPAL Collaboration;
L.A. del Pozo, University of Cambridge PhD thesis, RALT–002, 1993;
R. Akers *et al.*, OPAL Collaboration, Z. Phys. C63 (1994) 197.

19. B. Abbott, M. Bhattarcharjee, D. Elvira, F. Nang and H. Weerts, 'Fixed Cone Jet Definitions in DØ and R_{sep}' Fermilab–Pub–97/242–E.

20. J.E. Huth *et al.*, in *Research Directions for the Decade*, Proceedings of the Summer Study on High Energy Physics, Snowmass, Colorado, 1990, p. 134.

21. S.D. Ellis and D.E. Soper, Phys. Rev. D48 (1993) 3160.

22. M. Klasen and G. Kramer, 'Jet Shapes in ep and $p\bar{p}$ Collisions in NLO QCD', hep-ph/9701247.

23. H. Kuijf, 'NJETS: A Monte Carlo for QCD Backgrounds', unpublished;
F.A. Berends and H. Kuijf, Nucl. Phys. B353 (1991) 59.

24. Yu.L. Dokshitzer, V.A. Khoze, A.H. Mueller and S.I. Troyan, *Basics of Perturbative QCD*, Editions Frontières, Paris, 1991.

25. M.H. Seymour, Nucl. Phys. B421 (1994) 545.

26. H.L. Lai *et al.*, CTEQ Collaboration, Phys. Rev. D55 (1997) 1280.

27. S. Catani and B.R. Webber, University of Cambridge preprint Cavendish–HEP–97/10, in preparation.

28. Yu.L. Dokshitzer and B.R. Webber, Phys. Lett. B352 (1995) 451.

29. G. Turnock, 'Energy-Energy Correlation Distribution in e^+e^- Annihilation', University of Cambridge preprint Cavendish–HEP–92/3, unpublished.

30. P.E.L. Rakow and B.R. Webber, Nucl. Phys. B187 (1981) 254.

31. Yu.L. Dokshitzer and B.R. Webber, 'Power Corrections to Event Shape Distributions', hep-ph/9704298.

32. B.R. Webber, 'Hadronization', lectures given at Summer School on *Hadronic Aspects of Collider Physics*, Zuoz, Switzerland, 1994, hep-ph/9411384.

33. D.E. Soper, 'Jet Observables in Theory and Reality', hep-ph/9706320.